

Notes for the MIT NUPAX Oral Exam: Particle Physics

Siddharth Narayanan, MIT

Last modified: May 13, 2016

Disclaimer: the author of these notes makes no guarantee that anything in here is remotely correct.

Contents

0 General and miscellaneous information	6
0.1 Particles of the standard model	6
0.1.1 The J/ψ meson	9
0.2 Fermi's golden rule	9
0.3 Chirality	10
0.4 Other stuff	10
1 Discrete symmetries	11
1.1 Parity	11
1.2 CPT	11
2 Flavor symmetry and the quark model	12
2.1 Isospin and flavor symmetry	12
2.2 Building baryons and mesons	12
2.2.1 Baryons (ud) in the ground state	12
2.2.2 Mesons	13
2.3 SU(3) flavor symmetry	13
2.4 Light uds mesons	14
2.4.1 $l = 0$	14
2.5 Light uds baryons	15
2.5.1 Baryon magnetic moment	16
3 QCD and SU(3)	16
3.1 Color confinement	17
3.2 Running of α_S	18
4 Electron-positron annihilation	19
5 Electron-proton scattering (elastic)	20
5.1 Form factors	21
5.2 The Rosenbluth formula	21
6 Electron-proton scattering (inelastic)	22
6.1 Lorentz-invariant kinematic variables	22
6.2 Structure functions	23
6.3 Bjorken scaling and the Callan-Gross relation	23
6.4 Quarks and partons	24
6.4.1 Parton distribution functions	24
6.4.2 Sea quarks	25
6.5 HERA	25
6.5.1 Violation of Bjorken scaling	26
6.5.2 Global PDF fits	26
6.6 EMC effect and nuclear shadowing	27
6.7 Spin crisis	27
7 The weak interaction	27
7.1 Parity violation and the $V - A$ structure	27
7.1.1 Parity violation	27
7.1.2 $V - A$ structure	28
7.2 Weak boson kinematics	28

7.3	Pion decay	29
8	Weak interactions of leptons	29
8.1	Neutrino scattering	30
8.1.1	Nucleon cross-sections	30
8.1.2	Neutrino DIS	30
8.1.3	Weak contributions to e - p scattering	31
9	Neutrinos and oscillations	32
9.1	Solar neutrinos	32
9.1.1	Experimental detection	33
9.2	Mass and weak eigenstates	34
9.2.1	Example: oscillation between two flavors	34
9.2.2	Oscillation between three flavors	35
9.2.3	Neutrino masses	36
9.2.4	CP violation	36
9.3	MSW effect	36
10	Oscillation experiments	37
10.1	Reactor experiments	37
10.1.1	Short baseline	38
10.1.2	Long baseline	39
10.2	Global picture	39
11	Weak interactions of quarks	39
11.1	CP violation and baryogenesis	39
11.2	Cabbibo mixing and the weak interaction	40
11.3	The CKM matrix	41
11.4	Neutral kaon system	41
11.4.1	Kaon CP eigenstates	42
11.4.2	Kaon decays to pions	42
11.4.3	CP violation in kaons	43
11.5	Kaon oscillation	43
11.5.1	CPLEAR detector	44
11.5.2	Experimental discovery of neutral kaon oscillation	45
11.5.3	Measurement of CP violation	46
11.6	B -meson physics	46
11.6.1	BaBar detector	47
11.6.2	Experimental measurement of B^0 oscillation	48
11.6.3	CP violation in the neutral B system	49
12	Electroweak unification	50
12.1	W boson properties	50
12.2	The gauge structure: $SU(2)_L$	51
12.3	Electroweak unification	51
12.4	Experimental measurements of electroweak theory	52
12.4.1	Discovery of W and Z bosons	52
12.4.2	Measurement of the Z peak	52
12.4.3	Measurement of W properties	53
12.4.4	Measurement of t -quark properties	54

13 The Higgs boson	54
13.1 The Higgs mechanism in the Standard Model	54
13.2 Gauge boson masses and interactions	56
13.3 Fermion masses and interactions	56
13.4 Decays of the Higgs boson	56
13.5 Experimental discovery	57
14 Dark matter	57
14.1 Astrophysical evidence for DM	57
14.2 Candidates	58
14.3 Overview of searches	59
14.4 Direct detection	59
14.4.1 Cross-sections	60
14.4.2 Backgrounds	61
14.4.3 Detector types	62
14.4.4 Direct detection limits	62
15 Large Underground Xenon experiment	63
15.1 Signal signature	64
15.2 Detector components	64
15.2.1 Water tank and muon tagging	64
15.2.2 Cryogen	65
15.2.3 Xenon	65
15.2.4 TPC \vec{E} -field	65
15.2.5 PMTs and light collection	66
15.2.6 Triggering	66
15.3 Background sources and rejection	66
15.3.1 Electron recoils	66
15.3.2 Non-DM nuclear recoils	67
15.4 2013 results	67
16 Non-DM BSM	68
17 Nuclear physics	69
17.1 β^- decay	69
17.2 Nuclear isospin	69
17.3 NN interactions	70
17.4 Nuclear models	70
17.4.1 Liquid drop model	71
17.4.2 Shell model	71
17.4.3 Fermi gas model	72
17.5 Solar processes	72
17.5.1 PP processes	72
17.5.2 CNO cycle	73
17.6 Nucleosynthesis	73
17.6.1 BBN	73
17.6.2 Stellar	73
17.6.3 Supernovae	74
17.7 Quark-gluon plasma	74
17.7.1 RHIC	74
17.8 Nuclear reactors	75

Appendices**75****A Bibliography****75**

0 General and miscellaneous information

0.1 Particles of the standard model

Table of leptons in the Standard Model

Particle	Mass	Lifetime	Discovery
Electron	0.511 keV	Stable	CRT experiment led by J. J. Thomson in 1896
Muon	105 MeV	2.2×10^{-6} s 3×10^{10} eV	Discovered by in 1936 by looking at cosmic rays. Found they curved less sharply than electrons in a \vec{B} -field
Tau	1.76 GeV	2.9×10^{-13} s 2×10^{-3} eV	Discovered in $e^-e^+ \rightarrow e^\pm + \mu^\mp + \#$ events ($\tau\tau$ production) at SLAC.
Electron neutrino	-	-	Inferred from continuous spectrum of electron energy in β -decay. Directly observed in I β D using reactor antineutrinos.
Muon neutrino	-	-	Used $\pi \rightarrow \mu^- \bar{\nu}$ beam, and detected $\bar{\nu}_\mu p \rightarrow \mu^+ n$ events. The fact that only μ^+ (and not e^-) was observed implied $\nu_\mu \neq \nu_e$.
Tau neutrino	-	-	DONuT in 2000. Protons to charmed mesons to ν_τ (plus other stuff). Pass beam through magnets and shielding. Signature in detector is the appearance of a track (τ from CC interaction) and then a kink in the track (decay of τ)

Table of quarks in the Standard Model

Particle	Mass	Lifetime	Discovery
Up quark	2.3 MeV	-*	Inferred from success of quark model in describing baryon spectrum and DIS
Down quark	4.8 MeV	-*	Inferred from success of quark model in describing baryon spectrum and DIS
Strange quark	95 MeV	-*	Inferred from success of quark model in describing baryon spectrum and DIS
Charm quark	1.3 GeV	-*	Inferred from GIM mechanism ($K^0 \rightarrow \mu^+ \mu^-$ suppression). Direct discovery was J/ψ .
Bottom quark	4.2 GeV	-*	Inferred from CP violation in quark-weak interactions. Discovered in $\Upsilon(1S)$ [9.5 GeV] state using p -nucleus collisions.
Top quark	173 ± 0.5 GeV	3.3×10^{-25} s 2 ± 0.5 GeV	Discovered in $t\bar{t}$ production at Tevatron.

*Hadronizes before decay

Table of bosons in the Standard Model

Particle	Mass	Lifetime	Discovery
γ	0	Stable	First person to open his eyes
W^\pm	80 ± 0.015 GeV	2.1 ± 0.042 s	$p\bar{p}$ collisions at SPS (UA1 and UA2). Discovery was leptonic channels.
Z	91 ± 0.0021 GeV	2.5 ± 0.0023 s	$p\bar{p}$ collisions at SPS (UA1 and UA2).
H	125.1 ± 0.2 GeV	4 MeV [theory]	pp collisions at LHC (CMS and ATLAS).

Table of some mesons in the Standard Model

Particle	J^P	Mass	Lifetime	Discovery
$\pi^0(u\bar{u} - d\bar{d})$	0^-	135 MeV	8.4×10^{-17} s	1950: $\pi^0 \rightarrow \gamma\gamma$ at a collider.
$\pi^\pm(u\bar{d})$	0^-	139 MeV	2.6×10^{-8} s	1947: looking at cosmic rays in a emulsion detector.
$K^0(d\bar{s})$	0^-	497 MeV	9×10^{-11} s (K_S) 5×10^{-8} s (K_L)	
$K^\pm(u\bar{s})$	0^-	493 MeV	1.2×10^{-8} s	
$\eta(u\bar{u} + d\bar{d} - 2s\bar{s})$	0^-	547 MeV	5×10^{-19} s	
$\rho^0(u\bar{u} - d\bar{d})$	1^-	775 MeV	4.5×10^{-24} s	
$\rho^\pm(u\bar{d})$	1^-	775 MeV	4.5×10^{-24} s	
J/ψ	1^-	3.1 GeV	7.2×10^{-21} s	At BNL: using 28 GeV p beam on a Be target, using e^-e^+ final state. At SLAC: using e^-e^+ collisions, using hadrons/ $e^-e^+/\mu^+\mu^-$ final states
$\Upsilon(1S)$	1^-	9.5 GeV	1.2×10^{-20} s	At Fermilab using p -nucleus collisions
$B^0(d\bar{b})$	0^-	5.3 GeV	1.5×10^{-12} s	
$B^\pm(u\bar{b})$	0^-	5.3 GeV	1.6×10^{-12} s	
$B_s^0(s\bar{b})$	0^-	5.4 GeV	1.5×10^{-12} s	

0.1.1 The J/ψ meson

- Mass is 3.1 GeV and width is 93 keV.
 - Width is small relative to the $\phi(s\bar{s})$ because $\phi \rightarrow KK$ is possible but $J/\psi \rightarrow DD$ is not ($m_D \sim 1.9$ GeV)
 - Therefore, J/ψ must decay electromagnetically (small coupling constant) or through 3 gluons (OZI suppressed)
 - Same is true for the $\psi'(2S)$ state, but not for higher excited states since $m_{\psi''} > 2m_D$
- Discovered at SLAC and BNL
- The BNL experiment involved a p beam on a Be target

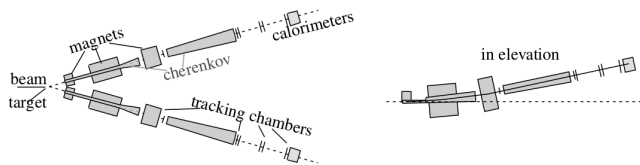


Fig. 4.22. The Brookhaven double-arm spectrometer. (Aubert *et al.* 1974 © Nobel Foundation 1976)

- To reconstruct mass, need $p_{e^\pm}, \theta_{e^\pm}$. $\theta = 14.6^\circ$ is fixed from the position of detectors
- Each detector picks up exactly one electron
- Momentum is measured using magnets that curve in the vertical direction
- Strength of the magnetic field is tuned to accept specific values of p to the rest of the detector
- Used a threshold Cerenkov and calorimeter to reject hadrons
- SLAC (SPEAR):
 - General purpose detector: tracking chambers (prop counters) and MWPCs
 - SPEAR scanned \sqrt{s} up to 8 GeV, enabling them to find higher excited states of ψ

0.2 Fermi's golden rule

- The decay rate is given by:

$$\Gamma_{fi} = 2\pi |T_{fi}|^2 \rho(E_i) \quad (1)$$

where $T_{fi} = \langle f | H_{\text{int}} | i \rangle$ (at LO) and $\rho(E_i)\delta E$ is the density of states with $E \in [E_i, E_i + \delta E]$

- We can write the density of states as the conservation of energy:

$$\rho(E_i) = \frac{dn}{dE} \Big|_{E=E_i} = \int dE_f \frac{dn}{dE_f} \delta(E_f - E_i) \quad (2)$$

- We can write the matrix element for normalized wavefunctions as as:

$$\mathcal{M}_{fi} = \int \psi_1, \psi_2, \dots |H_{\text{int}}| \psi_a, \psi_b, \dots \rangle = (2E_1 \cdots 2E_a \cdots)^{1/2} T_{fi} \quad (3)$$

where $\int d^3x |\psi|^2 = 2E$

- The differential cross-section is defined as:

$$\frac{d\sigma}{d\Omega} = \frac{N(\text{scattered into } d\Omega)}{\delta t \times N(\text{targets}) \times N(\text{incident particles per unit time per unit area})} \quad (4)$$

- The total cross-section is given by:

$$\sigma = \int \left(\prod_{i=1}^N \frac{d^3 \mathbf{p}_i}{2E_i(2\pi)^3} \right) \left(\prod_{j=1}^M \frac{d^3 \mathbf{k}_j}{2E_j(2\pi)^3} \right) \times |\mathcal{M}_{fi}|^2 \times \delta^4 \left(\sum p_i - \sum k_j \right) \quad (5)$$

- Cross sections are typically reported in barns $1 = 10^{-24}$ cm². The pp cross section is $\mathcal{O}(10)$ mb. $\sigma_{pp} < \sigma_{p\bar{p}}$ for $\sqrt{s} \lesssim 20$ GeV,

0.3 Chirality

- The chirality operators are

$$P_R = \frac{1}{2} (1 + \gamma^5), \quad P_L = \frac{1}{2} (1 - \gamma^5) \quad (6)$$

- Note $P_R + P_L = I$
- $P_{R,L}$ projects u onto $u_{R,L}$ and v onto $v_{L,R}$ (note the action is reversed for antiparticles)
- In the massless (relativistic) limit, chirality becomes helicity ($\vec{\sigma} \cdot \vec{p}/|\vec{p}|$)

0.4 Other stuff

- Synchrotron radiation is $\Delta E/\text{turn} \propto 1/m^4$
- Rapidity and pseudorapidity are defined by:

$$y = \frac{1}{2} \ln \frac{E + p_z}{E - p_z} \xrightarrow{m \rightarrow 0} \eta = -\ln \tan \frac{\theta}{2} \quad (7)$$

- Instantaneous luminosity is:

$$\mathcal{L} = f \frac{n_1 n_2}{A} \quad (8)$$

where f is the bunch crossing frequency; n_1, n_2 are the number of particles per bunch; A is the cross-sectional area of beams

- pp inclusive interaction cross section is \sim mb
- Jet algorithms are ways of reconstructing hadronization of colored particles:

- Cone algorithm:

1. Pick the highest p_T particle, collect all particles within $\Delta R < R_0$ of this seed. Add up the momenta of this cone and call it a candidate jet
2. If $\Delta R(\text{jet}, \text{seed})$ is less than some cutoff, then accept the candidate jet and remove all associated particles from the event.
3. Otherwise, repeat the cone process using the candidate jet axis as the new seed
4. After a candidate jet is accepted, remove all the associated particles from the event and return to step 1. The process ends when all particles are clustered

- Recursive algorithms:

- * Start with a particle i (typically highest p_T)
- * For $j \neq i$, compute:

$$d_{ij} = \min \left(k_{T,i}^{2\alpha}, k_{T,j}^{2\alpha} \right) \frac{\Delta R_{ij}}{R_0}, \quad d_{iB} = k_{T,i}^{2\alpha} \quad (9)$$

- * If $d_{iB} < d_{ij}$, then remove the particle from the event and call it a jet

- * Otherwise, choose the j' that minimizes d_{ij} . Add particles i and j' into a single particle and repeat the above steps
- * Proceed until all particles are clustered
- If we choose $\alpha = 1$, we get the k_T algorithm, which approximates the inversion of the QCd branching process
- $\alpha = -1$ is the anti- k_T algorithm, which produces circular jets
- $\alpha = 0$ is the Cambridge-Aachen algorithm and only relies on geometrical information

1 Discrete symmetries

1.1 Parity

- The parity operator flips space dimensions:

$$P\psi(\vec{x}, t) \mapsto \psi(-\vec{x}, t) \quad (10)$$

- Clearly P is hermitian and unitary

- For Dirac spinors, $P = \gamma^0 = \begin{pmatrix} I & \\ & -I \end{pmatrix}$

- Parity is conserved in QED:

- Matrix element for $e^- q \rightarrow e^- q$ scattering is:

$$\mathcal{M} = \frac{Q_q e^2}{q^2} j_e \cdot j_q, \quad j_x^\mu = \bar{u}(p_{x,f}) \gamma^\mu u(p_{x,i}) \quad (11)$$

- Applying P to the spinors:

$$u \rightarrow \gamma^0 u, \quad \bar{u} = u^\dagger \gamma^0 \rightarrow u^\dagger \gamma^{0\dagger} \gamma^0 = \bar{u} \gamma^0 \quad (12)$$

- So the currents transform as (k is a spatial coordinate):

$$j_x^0 \rightarrow j_x^0, \quad j_x^k \rightarrow -j_x^k \quad (13)$$

- The minus sign in the spatial component cancels when taking the inner product, so $P : \mathcal{M} \mapsto \mathcal{M}$

- Consider the decay of $\rho^0(1^-)$ to a pair of charged pions (0^-).

- Because the decay starts in the $J = 1$ state, the orbital angular momentum of the pion system must be 1. ($P = (-1)^l = -1$)
- This decay is allowed, since parity is conserved: $P(\rho^0) = P(\pi^+)P(\pi^-)(-1)^l = -1$

- Now consider the decay of $\eta(0^-)$ to a pair of charged pions

- The final orbital angular momentum is $l = 0$
- This decay is forbidden, since parity is violated: $P(\eta) \neq P(\pi^+)P(\pi^-)(-1)^l = 1$

- \Rightarrow parity is not conserved in the weak interaction

1.2 CPT

- In general, Lorentz-invariant QFTs must be invariant under CPT

- This is why particles have identical masses and magnetic moments

2 Flavor symmetry and the quark model

2.1 Isospin and flavor symmetry

- The nuclear force (i.e. residual strong force) is approximately charge-independent:

$$V_{pp} \sim V_{np} \sim V_{nn} \quad (14)$$

- The masses of the neutron and proton are very close
- Motivates an approximate symmetry for the strong interaction, known as (nuclear) isospin rotations. Define the proton as the isospin-up state and the neutron as the isospin-down state
- The same idea can be extended to quarks
 - If we assume that the EM strength for quarks in baryons is much weaker than the strong interaction, then we can impose an (approximate) symmetry for rotations in $q = \begin{pmatrix} u \\ d \end{pmatrix}$ space
 - Symmetry is approximate even if we drop the EM interaction since $m_u \neq m_d$
 - This is the isospin $\mathcal{T} = \frac{1}{2}\boldsymbol{\sigma}$. The Hamiltonian is invariant under rotations by $\exp[i\boldsymbol{\alpha} \cdot \mathcal{T}]$, for a real vector $\boldsymbol{\alpha}$.
 - T_i therefore generate the $\mathfrak{su}(2)$ Lie algebra
- We know bound states must consist of 2 or 3 quarks
 - Adding two isospin-half states gives an isospin triplet ($T = 1$) and an isospin singlet ($T = 0$)
 - Adding three isospin-half states gives an isospin quadruplet ($T = 3/2$) and *two* isospin doublets ($T = 1/2$). Note that the doublets are not states of definite symmetry
 - * However, one of the isospin doublets is symmetric under $1 \leftrightarrow 2$ (the 1, 2 system has isospin 1), so call it $\phi_S(\frac{1}{2}, T_3)$
 - * The other isospin doublet is antisymmetric under $1 \leftrightarrow 2$ (the 1, 2 system has isospin 0), so call it $\phi_A(\frac{1}{2}, T_3)$
 - Spin states also decompose in the same way (since spin is also SU(2))
- Antiquark isospin
 - Want to define an antiquark vector \bar{q} such that it transforms in the same way as q . That is:

$$q \rightarrow Uq \Rightarrow \bar{q} \rightarrow U\bar{q} \quad (15)$$

- This is done by defining $\bar{q} = \begin{pmatrix} -\bar{d} \\ \bar{u} \end{pmatrix}$.
- The ability to put q, \bar{q} in the same representation is special to SU(2)

2.2 Building baryons and mesons

2.2.1 Baryons (ud) in the ground state

- The total wavefunction looks like:

$$\psi = \text{flavor} \times \text{spin} \times \text{color} \times \text{space} \quad (16)$$

- It can be shown that the color wavefunction is always antisymmetric. If we only consider the $L = 0$ ground state, then the space wavefunction is symmetric ($(-1)^l$). Therefore, flavor \times spin must be symmetric, since the quarks are identical fermions (assuming the flavor symmetry)

- Ways of building symmetric $\phi_{\text{flavor}}\chi_{\text{spin}}$:

- Symmetric ϕ ($T = 3/2$) and symmetric χ ($S = 3/2$). This gives four distinct baryons (note \ni is used to describe the quark content without writing down the full wavefunction):

$$\Delta^- = ddd, \quad \Delta^0 \ni udd, \quad \Delta^+ \ni uud, \quad \Delta^{++} = uuu \quad (17)$$

- Using the symmetrized wavefunctions

$$\frac{1}{\sqrt{2}} \left[\phi_S \left(\frac{1}{2}, T_3 \right) \chi_S \left(\frac{1}{2}, S_3 \right) + \phi_A \left(\frac{1}{2}, T_3 \right) \chi_A \left(\frac{1}{2}, S_3 \right) \right] \quad (18)$$

The choice of T_3 gives two baryons:

$$p \ni uud, \quad n \ni udd \quad (19)$$

2.2.2 Mesons

- Bound state of a quark and antiquark \Rightarrow four possible isospin states
- The $T = 1$ states are the pions:

$$\pi^- = d\bar{u}, \quad \pi^0 = \frac{1}{\sqrt{2}}(u\bar{u} - d\bar{d}), \quad \pi^+ = u\bar{d} \quad (20)$$

2.3 SU(3) flavor symmetry

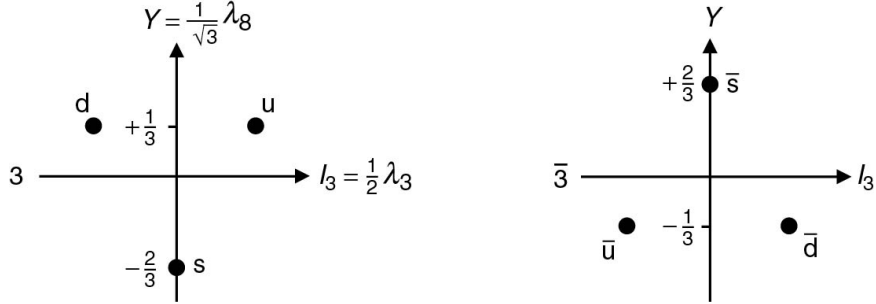
- ud symmetry can be extended to include strange quark
 - $m_s - m_{u/d} \sim 100$ MeV, which is not insignificant, but is small relative to binding energies of baryons \sim GeV
 - Strong hamiltonian is still invariant under uds , but the kinetic terms are less invariant than they were under the ud symmetry
 - Needs to be treated as an *approximate* symmetry
- Define the generators as $T_i = \frac{1}{2}\lambda_i$, where λ_i are the Gell-Mann matrices
 - $\lambda_{1,2,3}$ are the Pauli $\sigma_{1,2,3}$ matrices for the first two dimensions (i.e. u, d) \Rightarrow T_3 is still the third component of isospin. $T_3 s = 0$
 - $\lambda_{4,5,6,7}$ are (some of) the Pauli matrices for rotations between the other dimensions (i.e u, s and d, s)
 - Turns out that the 9 generators of the three SU(2) subgroups of SU(3) are not all independent. We allow u, d to retain all three of its generators and define λ_8 as a linear combination of the third generator for the other two subgroups
- Since $[T_3, T_8] = 0$, we define two (simultaneous) quantum numbers:

$$T_3 = \frac{1}{2}\lambda_3, \quad Y = \frac{1}{\sqrt{3}}\lambda_8 \quad (21)$$

where Y is the flavor hypercharge

- The remaining generators can be used to define ladder operators that step between $u \leftrightarrow d$, $d \leftrightarrow s$, $u \leftrightarrow s$

- The values of T_3, Y for the quarks and antiquarks make a triangle:

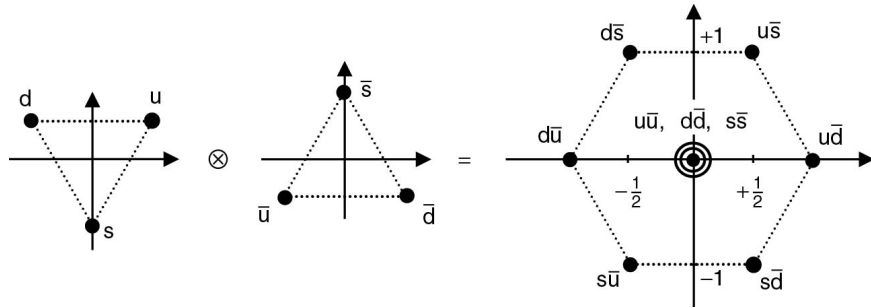


- To get the hadron masses described below (or something close), the following *constituent* masses are used:

$$m_u \approx m_d \approx 0.35 \text{ GeV}, \quad m_s \approx 0.5 \text{ GeV}, \quad m_c \approx 1.5 \text{ GeV} \quad (22)$$

2.4 Light uds mesons

- This diagram shows a cute way of writing down all $q\bar{q}$ combinations and getting their T_3, Y :



- Note that the three states in the middle are not physical (i.e. definite isospin)
- To get the physical states (linear combinations of $u\bar{u}, d\bar{d}, s\bar{s}$), we can act the raising/lowering operators on the edge states. This, however, only gives two linearly independent states
- Therefore, one of the linear combinations must be in a different rep of SU(3). It turns out the rep is the $T^2 = 0$ rep (here \mathcal{T} refers to the vector of SU(3) generators). The wavefunction is what one would expect:

$$\frac{1}{\sqrt{3}} (u\bar{u} + d\bar{d} + s\bar{s}) \quad (23)$$

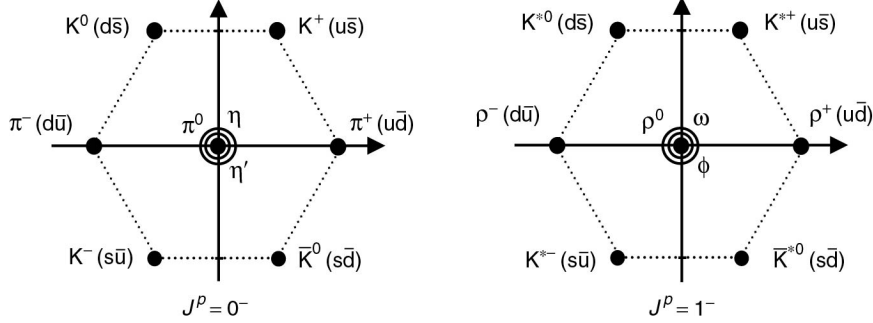
2.4.1 $l = 0$

- We now play the game of constructing the meson wavefunction (as was done for baryons). Note there are no Fermi statistics to deal with in this case
- We assume $l = 0$
- There are two possible spin states $s = 0, 1$. Since $l = 0$, we can say $J = 0, 1$.
- The parity of the meson is:

$$P(q\bar{q}') = +1 \times -1 \times (-1)^{l=0} = -1 \quad (24)$$

We therefore refer to $J^P = 0^-$ mesons as pseudoscalars and $J^P = 1^-$ as vectors (recall vectors have $P = -1$)

- The mesons are shown, split up by pseudoscalars (left) and vectors (right):



- The π^0 is as identified in $SU(2)$: $\frac{1}{\sqrt{2}}(u\bar{u} - d\bar{d})$. The η' has a high mass (~ 1 GeV) and corresponds to the singlet state identified above. Finally, the η is the remaining orthogonal state. Note these three physical states in reality have very different masses (which the $SU(3)$ theory does not predict) since $m_s \neq m_{u,d}$
- The prediction gets worse for the vector $T_3 = Y = 0$ states. We get (experimentally) the physical states:

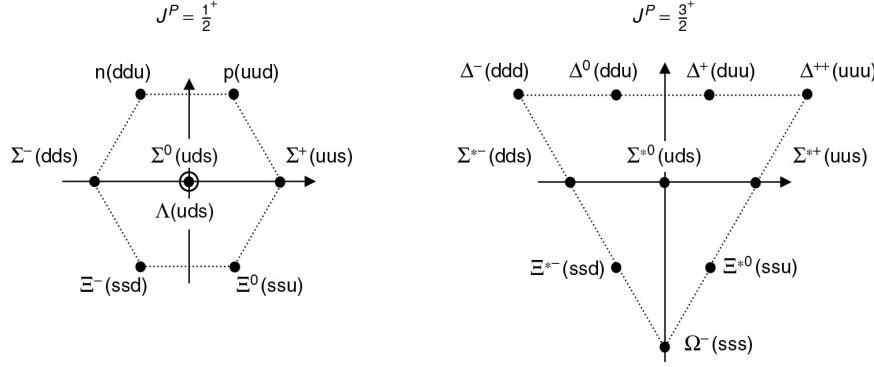
$$\rho^0 = \frac{1}{\sqrt{2}}(u\bar{u} - d\bar{d}), \quad \omega = \frac{1}{\sqrt{2}}(u\bar{u} + d\bar{d}), \quad \phi = s\bar{s} \quad (25)$$

Note the ρ^0 is kind of an excited state of the π^0

$J^P = 0^-$ meson	Mass [MeV]	$J^P = 1^-$ meson	Mass [MeV]
π^0	135	ρ^0	775
π^\pm	140	ρ^\pm	775
K^\pm	494	$K^{*\pm}$	892
K^0, \bar{K}^0	498	K^{*0}, \bar{K}^{*0}	896
η	548	ω	783
η'	958	ϕ	1020

2.5 Light uds baryons

- Once again, we assume $l = 0$
- Note that the parity for baryons is $+1 = (+1)^3 \times (-1)^{l=0}$
- The possible values of J^P therefore are $\frac{1}{2}^+, \frac{3}{2}^+$
- We can construct the following irreps by applying the $SU(3)$ ladder operators to $SU(2)$ extremal states:
 - A decuplet (which contains the deltas). It contains symmetric states. $T = 5/2$
 - Two octuplets of mixed symmetry. $T = 3/2$
 - A singlet which is totally antisymmetric. $T = 1/2$. Note: the state contains uds , so it cannot be created from a $SU(2)$ extremal state.
- Physical states must be antisymmetric in the quarks. Recall we need flavor \times spin to be symmetric. The result is:
 - A decuplet from the isospin decuplet
 - An octuplet formed from linear combinations of states in the two isospin octuplets
 - This exhausts everything except the isospin singlet state. However, there is no way to form a totally antisymmetric spin state out of three spin-half particles, so it does not correspond to a physical state



<i>s</i> quarks	Octet	Mass [GeV]	Decuplet	Mass [GeV]
0	p, n	0.94	Δ	1.2
1	Σ	1.2	Σ^*	1.4
1	Λ	1.1		
2	Ξ	1.3	Ξ^*	1.5
3			Ω	1.7

2.5.1 Baryon magnetic moment

- Define the nuclear magneton:

$$\mu_N = \frac{e\hbar}{2m_p} \quad (26)$$

- The magnetic moments for a baryon b is calculated by writing out the wavefunction $|b \uparrow\rangle$ in terms of the up/down states of the constituent quarks and computing:

$$\langle b \uparrow | \mu_z | b \uparrow \rangle \quad (27)$$

The quark magnetic moments are computed as:

$$\mu_q = \langle q \uparrow | \mu_z | q \uparrow \rangle = -\langle q \downarrow | \mu_z | q \downarrow \rangle \quad (28)$$

- The moments for protons and neutrons are:

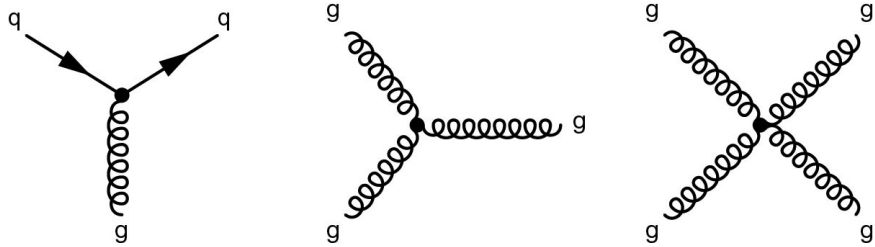
$$\mu_p = 2.79\mu_N, \quad \mu_n = -1.9\mu_N \quad (29)$$

3 QCD and SU(3)

- QCD is the QFT of the strong interaction
- Mediated by gluons, which are massless gauge bosons corresponding to a local SU(3) symmetry
- Quarks lie in the fundamental rep of SU(3). The three basis vectors are labeled red, blue, green, and the generators are the usual Gell-Mann matrices:

$$T^a = \frac{1}{2}\lambda_a \quad (30)$$

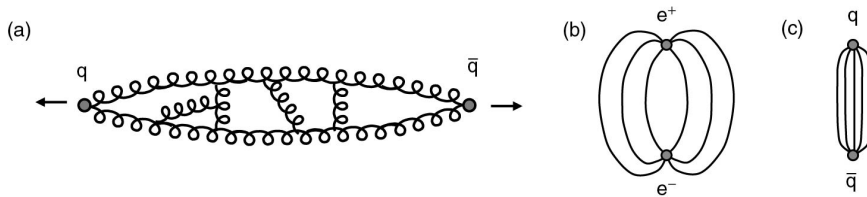
- Antiquarks are in the adjoint rep and the basis vectors are $\bar{r}, \bar{g}, \bar{b}$
- Because SU(3) is non-Abelian, there are gluon self-interactions:



- There are 8 physical gluon states, corresponding to the 8 Gell-Mann matrices
 - 6 are of the form $c\bar{c}'$, where c, c' are distinct colors
 - The other two correspond to λ_3, λ_8 and are $\frac{1}{\sqrt{2}}(r\bar{r} - g\bar{g})$ and $\frac{1}{\sqrt{6}}(r\bar{r} + g\bar{g} + 2b\bar{b})$

3.1 Color confinement

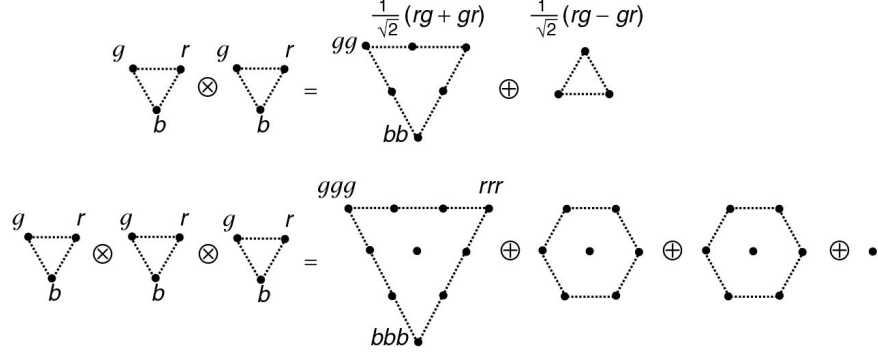
- Particles must always exist in color singlet states
- Has not been proven theoretically, but a qualitative argument can be made:
 - Unlike the \vec{E} -field of two charges being pulled apart, the strong field lines do not spread apart in space, due to gluon self-interaction:



- Therefore, the energy grows linearly with the distance (experimentally ~ 1 GeV/fm)
- Gluons split into quarks, making color singlet states
- Implies gluons cannot travel over macroscopic distances, as they carry color
- As with flavor SU(3) symmetry, can define two quantum numbers T_3^c, Y^c to characterize color SU(3) symmetry.
 - Adding two quarks together gives an octuplet and a singlet:

$$\begin{array}{c}
 \text{Diagram showing the tensor product of two quark lines (g and r) and their antiquarks (bar{b} and bar{g}) to form an octuplet and a singlet.} \\
 \otimes \\
 \text{Diagram showing the tensor product of two antiquark lines (bar{r} and bar{b}) to form an octuplet and a singlet.} \\
 = \\
 \text{Diagram showing the resulting tensor product of all four lines (g, r, bar{b}, bar{g}) to form an octuplet and a singlet.} \\
 \oplus \\
 \frac{1}{\sqrt{3}}(r\bar{r} + g\bar{g} + b\bar{b})
 \end{array}$$

- Similarly, adding three quarks (or three antiquarks) gives a decuplet, two octuplets, and a singlet:



- Only the singlet states correspond to physical states

- Hadronization

- If two quarks are produced (say $\gamma \rightarrow q\bar{q}$) and the quarks have high energy, they will fly apart
- However, the interaction of the gluon field between them has a high energy density (1 GeV/fm), and so the gluons split into quarks
- This process repeats until all of the quarks are bound in color singlet states

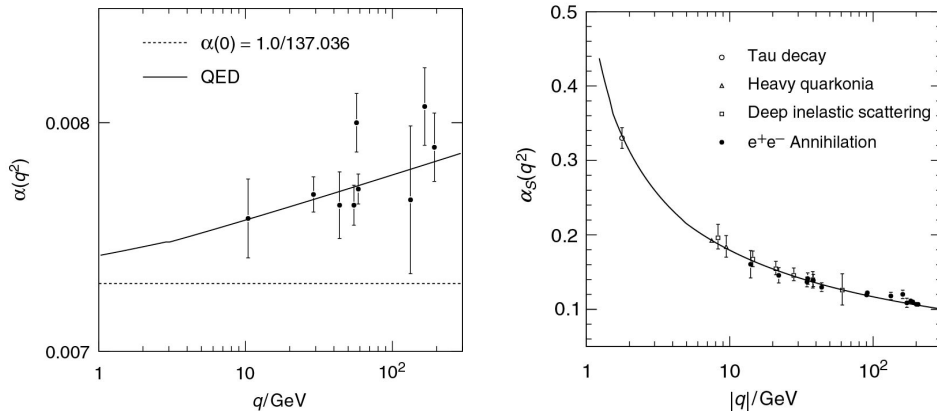
3.2 Running of α_S

- Coupling constants run due to higher order corrections made to boson propagators
 - The size of these corrections is necessarily dependent on q^2
 - We absorb this q^2 dependence into the coupling constant, e.g. $\alpha \rightarrow \alpha(q^2)$, $\alpha_S \rightarrow \alpha_S(q^2)$
- At low energies, $\alpha_S \sim \mathcal{O}(1)$
- Because of the non-Abelian structure of gluon interactions, the q^2 evolution of α_S depends on

$$B = \frac{11N_c - 2N_f}{12\pi} \quad (31)$$

In the SM, $B > 0 \Rightarrow \alpha_S$ decreases as a function of q^2

- This is in contrast with QED, which gets stronger at short distances/high energies:



- At $q \sim 100$ GeV, QCD enters a perturbative regime
- Asymptotic freedom

- Explains why quarks in DIS experiments can be treated as free particles
- Running can be measured by looking at jet production at colliders
 - e.g. if the $e^-e^+ \rightarrow q\bar{q}$ and $e^-e^+ \rightarrow q\bar{q}g$ diagrams are included when calculating R (described next section), we get:

$$R \rightarrow \left(1 + \frac{\alpha_S(q^2)}{\pi}\right) \times 3 \sum_i Q_{q_i}^2 \quad (32)$$

giving a very precise measurement of $\alpha_S(q^2)$

4 Electron-positron annihilation

- First, the inclusive cross-sections for annihilation are (below the Z -peak):

$$\sigma(e^-e^+ \rightarrow \mu^-\mu^+) = \frac{4\pi\alpha^2}{s}, \quad \sigma(e^-e^+ \rightarrow q\bar{q}) = \frac{4\pi\alpha^2}{s} \times 3Q_q^2 \quad (33)$$

- The inclusive cross-section to hadrons is gotten by summing over all quark flavors satisfying $2m_q < \sqrt{s}$:

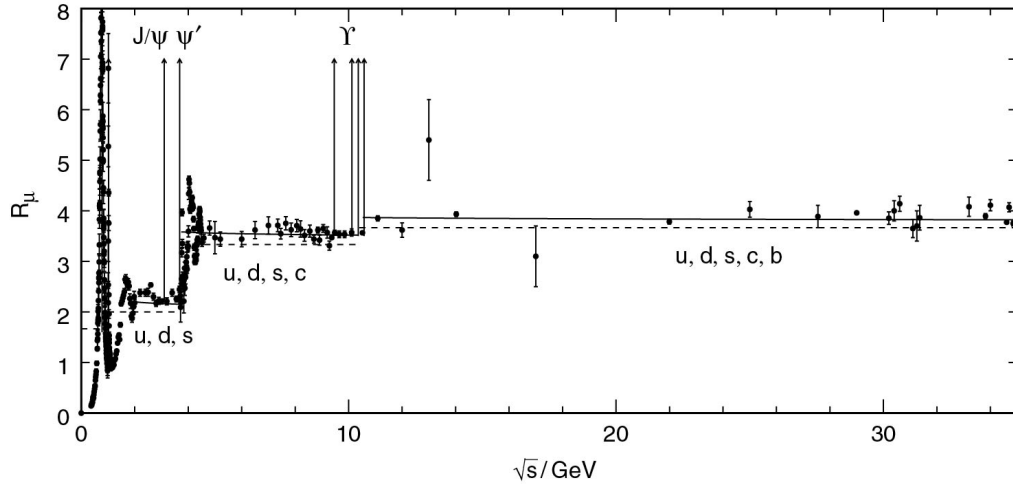
$$\sigma(e^-e^+ \rightarrow \text{hadrons}) = \sigma(e^-e^+ \rightarrow q\bar{q}) = \frac{4\pi\alpha^2}{s} \times 3 \sum_i Q_{q_i}^2 \quad (34)$$

- Dividing, we get the ratio:

$$R(s) = \frac{\sigma(e^-e^+ \rightarrow \text{hadrons})}{\sigma(e^-e^+ \rightarrow \mu^-\mu^+)} = 3 \sum_i Q_{q_i}^2 \quad (35)$$

For example, $R((2 \text{ GeV})^2) = 3 \times \left(\frac{3}{9} + \frac{1}{9} + \frac{1}{9}\right) = 2$

- A plot at low values of \sqrt{s} is:



The discrete jumps correspond to $\sqrt{s} = 2m_{q_i}$. The resonances are to $J^P = 1^-$ mesons (needs to be the same as the photon)

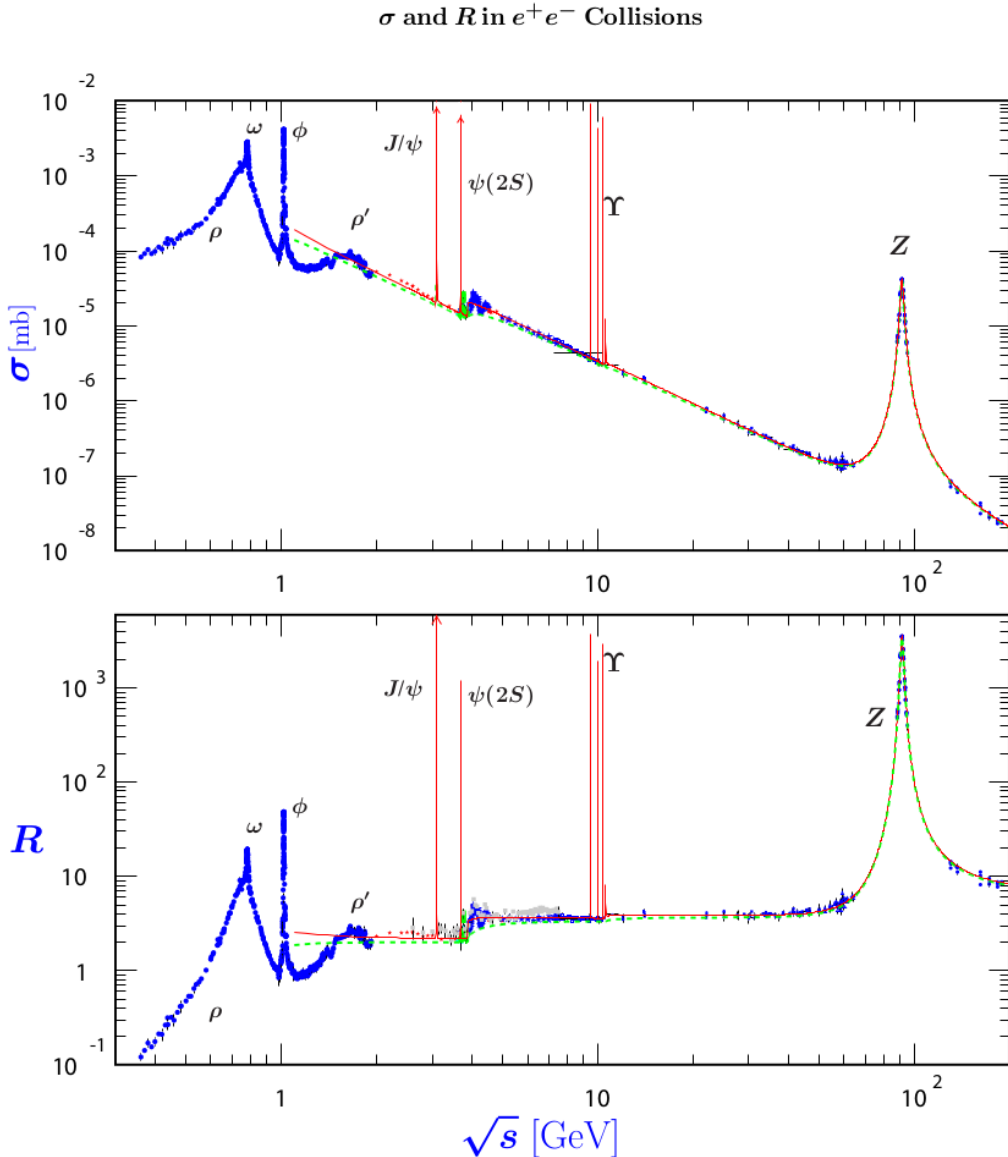
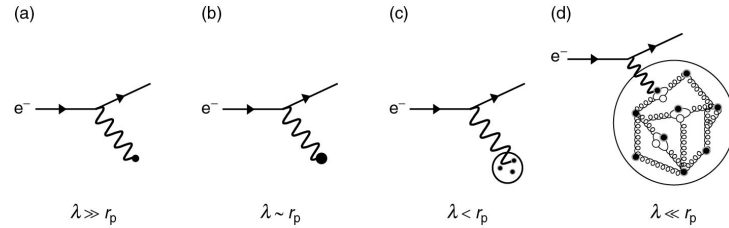


Figure 50.5: World data on the total cross section of $e^+e^- \rightarrow \text{hadrons}$ and the ratio $R(s) = \sigma(e^+e^- \rightarrow \text{hadrons}, s)/\sigma(e^+e^- \rightarrow \mu^+\mu^-, s)$. $\sigma(e^+e^- \rightarrow \text{hadrons}, s)$ is the experimental cross section corrected for initial state radiation and electron-positron vertex loops, $\sigma(e^+e^- \rightarrow \mu^+\mu^-, s) = 4\pi\alpha^2(s)/3s$. Data errors are total below 2 GeV and statistical above 2 GeV. The curves are an educative guide: the broken one (green) is a naive quark-parton model prediction, and the solid one (red) is 3-loop pQCD prediction (see “Quantum Chromodynamics” section of this *Review*, Eq. (9.7) or, for more details, K. G. Chetyrkin *et al.*, Nucl. Phys. **B586**, 56 (2000) (Erratum *ibid.* **B634**, 413 (2002)). Breit-Wigner parameterizations of J/ψ , $\psi(2S)$, and $\Upsilon(nS)$, $n = 1, 2, 3, 4$ are also shown. The full list of references to the original data and the details of the R ratio extraction from them can be found in [[arXiv:hep-ph/0312114](#)]. Corresponding computer-readable data files are available at <http://pdg.lbl.gov/current/xsect/>. (Courtesy of the COMPAS (Protvino) and HEPDATA (Durham) Groups, May 2010.)

5 Electron-proton scattering (elastic)



- The structure probed by the EM interaction depends on the energy of the e^- (which determines the Q^2 of

the interaction)

- At non-relativistic energies, the proton can be described as a point charge
- If $1/E_\gamma \sim r_p \sim 1$ fm, the proton is an extended charge with non-zero μ
- At $1/E_\gamma < r_p$, the valence quarks of the proton are probed
- And in the limit $1/E_\gamma \ll r_p$, the sea of quarks and gluons is probed
- Rutherford scattering
 - Non-relativistic limit of e^-
 - If T_e is the kinetic energy of the electron:

$$\frac{d\sigma}{d\Omega} = \frac{\alpha^2}{16T_e^2 \sin^4(\theta/2)} \quad (36)$$

- Mott scattering
 - The electron is relativistic, but not so high energy that we need to consider proton recoil, extended charge, etc
 - $m_e < E_e < m_p$

$$\frac{d\sigma}{d\Omega} = \frac{\alpha^2}{4E_e^2 \sin^4(\theta/2)} \cos^2 \frac{\theta}{2} \quad (37)$$

5.1 Form factors

- As E_γ increases, we need to account for the extended charge distribution
- Write the charge distribution as $Q\rho(\mathbf{r}')$. Then, the (classical) electric form factor is the Fourier transform of the charge distribution:

$$F(\mathbf{q}^2) = \int d^3r \rho(\mathbf{r}) e^{i\mathbf{q}\cdot\mathbf{r}} \quad (38)$$

- The differential cross-section becomes:

$$\left(\frac{d\sigma}{d\Omega} \right)_{\text{Mott}} \rightarrow \left(\frac{d\sigma}{d\Omega} \right)_{\text{Mott}} \times \left(F(\mathbf{q}^2) \right)^2 \quad (39)$$

5.2 The Rosenbluth formula

- We now write down the relativistic, leading-order, e^-p elastic scattering cross-section:

$$\frac{d\sigma}{d\Omega} = \frac{\alpha^2}{4E_1^2 \sin^4(\theta/2)} \frac{E_3}{E_1} \left(\frac{G_E^2 + \tau G_M^2}{1 + \tau} \cos^2 \frac{\theta}{2} + 2\tau G_M^2 \sin^2 \frac{\theta}{2} \right), \quad \tau = \frac{Q^2}{4m_p^2} \quad (40)$$

Recall $Q^2 = -q^2$

- The form factors $G_E(Q^2)$ and $G_M(Q^2)$ account for the extended charge and magnetic moment distributions inside the proton
- As discussed below, the anomalous magnetic moment of the proton is

$$\mu = 2.79 \frac{e}{m_p} \mathbf{S} \quad (41)$$

so naively, we can guess $G_M(Q^2) = 2.79G_E(Q^2)$

- The G_s can be measured experimentally.

– G_E as a function of Q^2 can be extracted by measuring the differential cross-section at low Q^2 and dividing by the expectation from the Mott formula:

$$\frac{d\sigma}{d\Omega} / \left(\frac{d\sigma}{d\Omega} \right)_{\text{Mott}} \approx G_E^2 \text{ at low } Q^2 \quad (42)$$

– Similarly, G_M can be extracted:

$$\frac{d\sigma}{d\Omega} / \left(\frac{d\sigma}{d\Omega} \right)_{\text{Mott}} \approx \left(1 + 2\tau \tan^2 \frac{\theta}{2} \right) G_M^2 \text{ at high } Q^2 \quad (43)$$

– Experiment verifies $G_M \approx 2.79G_E$

- By taking the Fourier transform of $G_E(Q^2)$ at low Q^2 , we can extract the charge distribution:

$$\rho(\mathbf{r}) \approx \rho_0 e^{-r/a}, \quad a = 0.24 \text{ fm} \quad (44)$$

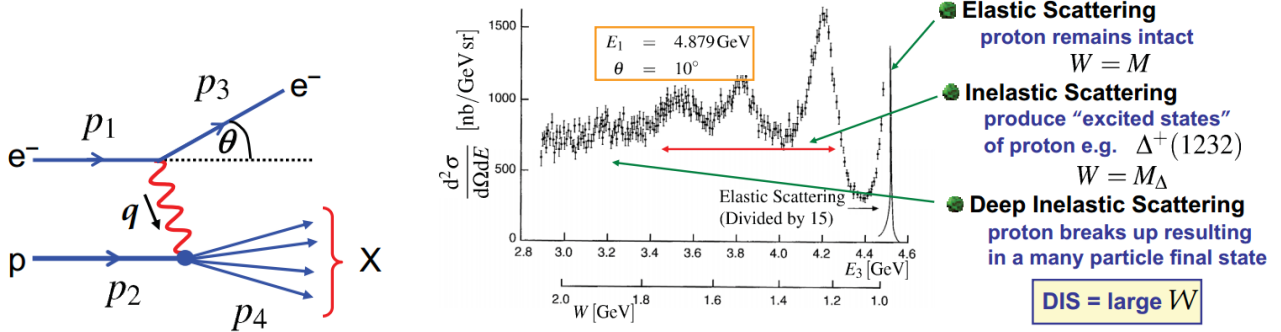
which gives a RMS of 0.8 fm

- At high Q^2 , the cross-section goes as:

$$\left(\frac{d\sigma}{d\Omega} \right)_{\text{elastic}} \propto \frac{1}{Q^6} \left(\frac{d\sigma}{d\Omega} \right)_{\text{Mott}} \quad (45)$$

so elastic scattering is very suppressed. This is because the proton has finite size and the form factors fall at high Q^2 . In inelastic scattering, the photon interacts with point particles, which do not have form factors.

6 Electron-proton scattering (inelastic)



6.1 Lorentz-invariant kinematic variables

- Q^2 is the energy transfer squared

$$Q^2 = -q^2 \quad (46)$$

The DIS regime is $Q^2 \gtrsim \text{few GeV}$

- Bjorken x is a measure of the elasticity

$$x = \frac{Q^2}{2p_2 \cdot q}, \quad x \in [0, 1] \quad (47)$$

Note $x = 1$ is the fully elastic scenario (the scattering is probing the proton as a whole)

- W is the mass of the hadronic final state

$$W^2 = p_4^2 \geq m_p^2 \quad (48)$$

The inequality is because the final state hadronic system must include at least one baryon, and the proton is the lightest baryon

- Inelasticity y :

$$y = \frac{p_2 \cdot q}{p_2 \cdot p_1}, \quad y \in [0, 1] \quad (49)$$

- ν

$$\nu = \frac{p_2 \cdot q}{m_p} \quad (50)$$

- The above quantities are obviously not all independent. Knowing two of them specifies the rest.
- “Higher twist” effects are $\mathcal{O}((\Lambda_{\text{QCD}}^2/Q^2))$

6.2 Structure functions

- Can write the DIS cross-section as

$$\frac{d^2\sigma}{dx dQ^2} = \frac{4\pi\alpha^2}{Q^4} \left[(1-y) \frac{F_2(x, Q^2)}{x} + y^2 F_1(x, Q^2) \right] \quad (51)$$

where F_i are the structure functions

- The double-differential cross-section can be measured easily at a fixed-target $e^- p$ scattering experiment, since Q^2, x, y are all determined by E_1, E_3, θ of the electron
 - Can also be done at non-fixed-target experiments; kinematics are just simpler in this case
 - $F_1(x, Q^2), F_2(x, Q^2)$ are extracted by looking events at fixed x, Q^2 , and varying y . The structure functions can then be extracted from the double-differential cross-section

6.3 Bjorken scaling and the Callan-Gross relation

- Experiments at SLAC did systematic study of F_i as functions of x, Q^2

- e^- beam (5-20 GeV) fired at liquid hydrogen target
- Used movable e^- spectrometer to scan θ

- Bjorken scaling is the observation:

$$F_1(x, Q^2) \sim F_1(x), \quad F_2(x, Q^2) \sim F_2(x) \quad (52)$$

- That is, the structure functions have weak Q^2 dependence
- Implies that whatever the photon is probing is point-like \Rightarrow evidence for quark model
- Scaling is violated at very high Q^2 (discussed below) \Rightarrow quark-gluon interactions
 - * At high Q^2 , higher-order QCD interactions become relevant, for example $q \rightarrow qg \rightarrow q$ loops

- The same experiments gave the Callan-Gross relation:

$$F_2(x) = 2xF_1(x) \quad (53)$$

- Holds true in the DIS regime for Q^2
- Implies that fundamental interaction is elastic scattering of spin-half particles (i.e. $e^-q \rightarrow e^-q$)

6.4 Quarks and partons

- The Bjorken x is the fraction of momentum carried by a parton in the “infinite momentum” frame.
 - In this frame, the proton momentum is $p^\mu = (p, p, 0, 0)$ (i.e. can ignore the mass)
 - Let ξ be the fraction of momentum held by the parton. The scattering process is:

$$\xi p^\mu \rightarrow \xi p^\mu + q^\mu \quad (54)$$

- Since the parton is on-shell before and after:

$$(\xi p)^2 = m_q^2 \quad (55)$$

$$(\xi p + q)^2 = \xi^2 p^2 + 2\xi p \cdot q + q^2 = m_q^2 \quad (56)$$

- Equating and solving for ξ gives:

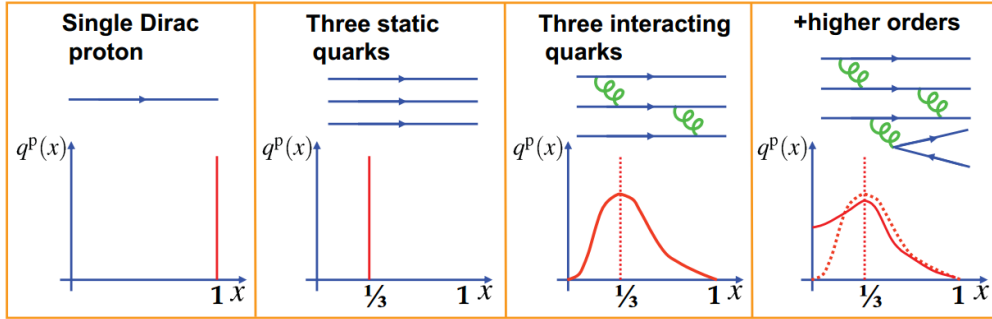
$$\xi = \frac{-q^2}{2p \cdot q} = \frac{Q^2}{2p \cdot q} = x \quad (57)$$

- The scattering off a spin-half point particle $e^- q \rightarrow e^- q$ can be written in terms of y and the parton’s charge Q_q :

$$\frac{d\sigma}{dQ^2} = \frac{4\pi\alpha^2 Q_q^2}{Q^4} \left[(1-y) + \frac{y^2}{2} \right] \quad (58)$$

6.4.1 Parton distribution functions

- Let $q_i^p(x)$ be the probability distribution function of the momentum fraction x held by quarks of flavor q_i in a proton



- The total ep scattering cross-section is gotten by convoluting the above formula for $d\sigma/dQ^2$ with the PDFs:

$$\frac{d^2\sigma^{ep}}{dx dQ^2} = \frac{4\pi\alpha^2}{Q^4} \left[(1-y) + \frac{y^2}{2} \right] \sum_q Q_q^2 q_i^p(x) \quad (59)$$

- We can recover the structure functions from this:

$$F_2^{ep}(x, Q^2) = 2xF_1^{ep}(x, Q^2) = x \sum_i Q_i^2 q_i^p(x) \quad (60)$$

Note that this directly predicts Bjorken scaling and the Callan-Gross relation

- Using isospin symmetry, we can define the PDFs for neutrons:

$$\begin{aligned} u^p(x) &= d^n(x) \equiv u(x) \\ d^p(x) &= u^n(x) \equiv d(x) \end{aligned} \quad (61)$$

and similarly for $\bar{u}(x), \bar{d}(x)$

- Define

$$f_q = \int dx x[q(x) + \bar{q}(x)] \quad (62)$$

f_u, f_d can be determined by measuring F_2^{ep}, F_2^{en} (neutron scattering is done on deuterium). We find:

$$f_u \approx 0.36, \quad f_d \approx 0.18 \quad (63)$$

in the proton. Therefore, nearly half of the momentum is held in gluons

6.4.2 Sea quarks

- The above discussion only considered uud (udd) in protons (neutrons). It can be extended to include sea quarks (considering only u, d now)

- First, define:

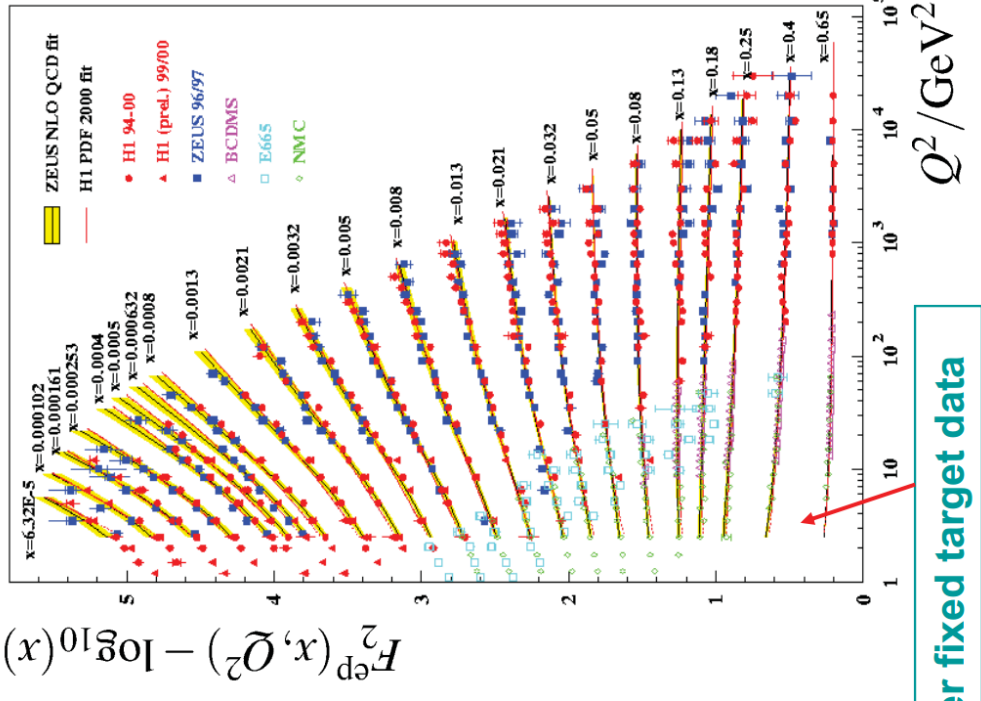
$$q(x) = q_V(x) + q_S(x), \quad \bar{q}(x) = \bar{q}_S(x) \quad (64)$$

- Since sea quarks are produced in pairs from gluon splitting, we can assume $q_S = \bar{q}_S$. Since the masses of the u and d are close enough on the DIS energy scale, we can also assume $u_S \approx d_S$
- We expect that at very low x , sea quarks will dominate the PDFs. In this case:

$$\lim_{x \rightarrow 0} \frac{F_2^{en}(x)}{F_2^{ep}(x)} = 1 \quad (65)$$

which was verified at SLAC

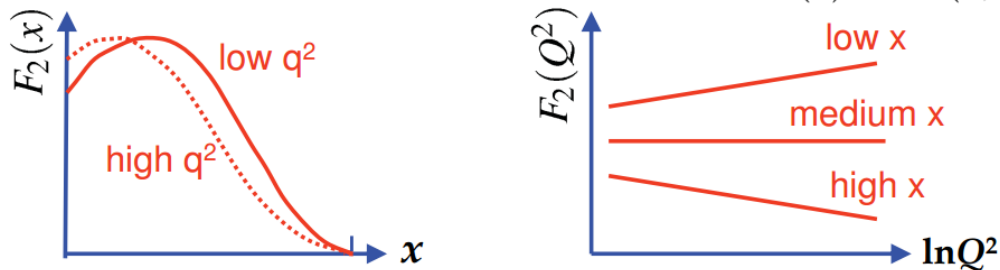
6.5 HERA



- 27.5 GeV e^-/e^+ beam colliding with a 820 or 920 GeV proton beam
- Detector is “forward” in the direction of the proton beam
- Measured parameters were e^- energy and scattering angle \Rightarrow sufficient to determine Q^2, x, y

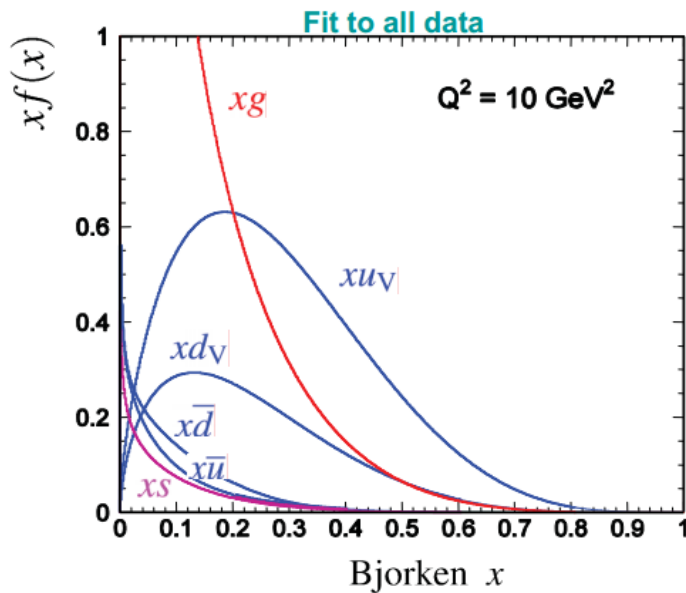
- Hadron shower used for trigger only
- Huge range of x, Q^2 was probed.
- Very powerful evidence of Bjorken scaling
 - There is a violation at low/high Q^2 , but not consistent across x
 - \Rightarrow quark radius is $< hc/Q \sim 10^{-18}$ m

6.5.1 Violation of Bjorken scaling



- At high Q^2 , the photon probes quarks at lower x , arising from diagrams like $q \rightarrow qg \rightarrow q$
- So at low x , the structure function goes up at high Q^2 ; at high x , the structure function goes down at high Q^2
- DGLAP equations describes Q^2 -dependence

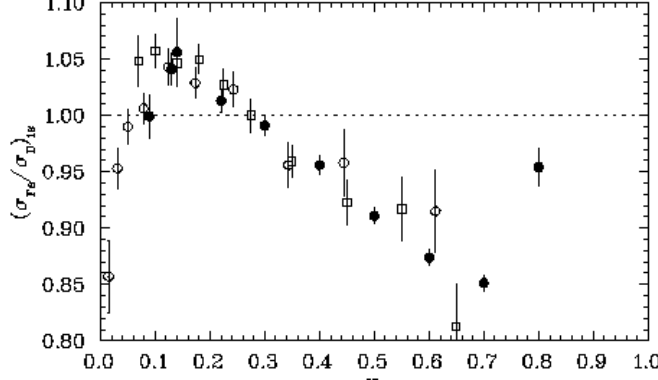
6.5.2 Global PDF fits



- Fit is done with information from multiple experiments
- Hadron colliders \Rightarrow gluon PDF
- Can use νN experiments to isolate interactions with u, d (depending on $\nu/\bar{\nu}$)

6.6 EMC effect and nuclear shadowing

Figure 1: $(\sigma_{F_\pi}/\sigma_D)$ ratios as a function of x from EMC (hollow circles), SLAC (solid circles), and BCDMS (squares). The data have been averaged over Q^2 and corrected for neutron excess (i.e. for isoscalar nuclei).



- Can measure $F_2^A(x)$ for various elements
- At low $x \lesssim 0.05$, we find there is lower cross section for e^-N scattering, so $F_2^A/F_2^D < 1$ (nuclear shadowing)
- At high $x \gtrsim 0.3$, we find that there is once again a lower cross section (relative to scattering off D). This is the EMC effect and not well-understood
 - Conclusion essentially is that we cannot treat nucleons in nucleus as independent, interacting particles

6.7 Spin crisis

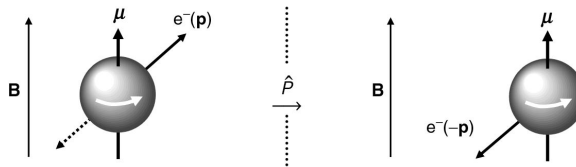
- Using polarized particles (polarized μ^- beam and p target by EMC), we can measure the spin of the proton constituents
- We find that the spin of valence quarks is only $1/4$ of proton spin
- RHIC is making measurements of gluon polarization using polarized p beams

7 The weak interaction

7.1 Parity violation and the $V - A$ structure

7.1.1 Parity violation

- Experimentally observed through the process $^{60}\text{Co} \rightarrow ^{60}\text{Ni}^* + e^- + \bar{\nu}_e$
 - Cobalt has permanent nuclear magnetic moment μ , so it can be aligned using an external B -field
 - Wu and collaborators found that the flux of electrons emitted in the same hemisphere as $\vec{\mu}$ (i.e. $\vec{\mu} \cdot \vec{p}_e > 0$) is much lower than the flux of electrons emitted in the opposite hemisphere
 - Under parity, $P : \vec{p} \mapsto -\vec{p}$. But since $\vec{B}, \vec{\mu}$ are axial vectors, they are invariant under parity. Therefore, the asymmetry represents violation of parity invariance.



7.1.2 $V - A$ structure

- Assuming that the weak interaction is mediated by a spin-1 boson, there are two possible currents: $\bar{\psi}\gamma^\mu\psi$ (vector) and $\bar{\psi}\gamma^\mu\gamma^5\psi$ (axial vector)
 - Most general form is a linear combination of the two: $j = g_V j_V + g_A j_A$
 - Can write out all the terms of $j_x \cdot j_y$ (where $x = \nu_e e^-$ and $y = du$ for example) and check the effect of P
 - The term that is not invariant under P has a relative strength of

$$\frac{g_V g_A}{g_V^2 + g_A^2} \quad (66)$$

– \Rightarrow Need $g_V, g_A \neq 0$ to get parity violation

- Experimentally, have found the structure to be:

$$j^\mu = \frac{g_W}{\sqrt{2}} \bar{u}(p') \frac{1}{2} \gamma^\mu (1 - \gamma^5) u(p) \quad (67)$$

i.e. $g_V = -g_A$

- Chirality consequences of interaction structure:

- Recall for QED that the spinors in particle current $\bar{u}\gamma^\mu u$ must be both right-handed or both left-handed
- The $1 - \gamma^5$ in the weak particle current acts as a P_L operator, so both spinors must be left-handed
- In the antiparticle current, both must be right-handed.
- Note this is also a consequence/cause of parity violation:
* $P : LH \rightarrow RH$, one of which interacts weakly while the other does not

7.2 Weak boson kinematics

- Propagator is:

$$\frac{-i}{q^2 - m_W^2} \left(g_{\mu\nu} - \frac{q_\mu q_\nu}{m_W^2} \right) \rightarrow \frac{-ig_{\mu\nu}}{q^2 - m_W^2} \quad (68)$$

where the limit is taken assuming $q \ll m_W$, which is generally valid for things like β -decay, ν DIS, etc.

- Fermi four-point interaction

- Can take the $q \ll m_W$ limit further, so the propagator becomes

$$\frac{ig_{\mu\nu}}{m_W^2} \quad (69)$$

- In this case, the interaction no longer depends on the kinematics of the W boson, so it can be treated as a four-point interaction
- Historically, it is written in terms of G_F , which is:

$$\frac{G_F}{\sqrt{2}} = \frac{g_W^2}{8m_W^2} \quad (70)$$

- Numerically, $G_F = 1.17 \times 10^{-5}$ GeV $^{-2}$

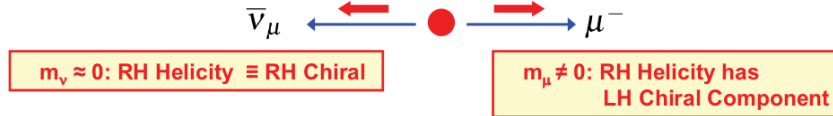
- The dimensionless coupling strength of the weak interaction is:

$$\alpha_W \equiv \frac{g_W^2}{4\pi} \approx \frac{1}{30} \quad (71)$$

which is an order of magnitude larger than α

7.3 Pion decay

- Consider the decay of the charged pion (at rest) $\pi^-(\bar{u}d) \rightarrow \ell \bar{\nu}_\ell$
- The charged pion is 0^- , so the ℓ and $\bar{\nu}_\ell$ must be in the spin-singlet state.
 - If we assume $m_\nu = 0$, a right-handed (chirality) $\bar{\nu}$ must also be right-handed (helicity)
 - Since the decay products are back-to-back, the ℓ must also be right-handed (helicity) to be in the spin-singlet state



- If $m_\ell = 0$, this decay would be forbidden, since only the left-handed (chirality) ℓ couples to the weak current. Since this is not the case, there is a small overlap between the right-handed (helicity) and left-handed (chirality) ℓ states
- The matrix-element of this decay is suppressed due to this small overlap:

$$\mathcal{M} \sim \frac{m_\ell}{m_\pi + m_\ell} \quad (72)$$

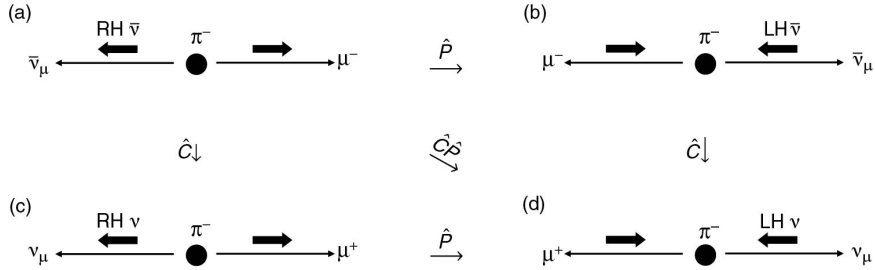
where $m_\pi = 140$ MeV

- Since $m_\mu/m_e \sim 200$, the decay to muons is heavily favored.
 - Note that $m_e \ll m_\pi$ is what really drives the suppression, since the electron must be highly relativistic due to the mass difference \Rightarrow right-handed (helicity) is almost entirely right-handed (chirality)
- The decay rate is proportional to:

$$\Gamma(\pi^- \rightarrow \ell \bar{\nu}_\ell) \propto \left(m_\ell (m_\pi^2 - m_\ell^2) \right)^2 \quad (73)$$

So $\Gamma(e)/\Gamma(\mu) \sim 10^{-4}$

- Note that this example shows that the weak interaction violates P and C , but not CP . Consider $\pi^- \rightarrow \bar{\nu}_\mu \mu^-$, where the $\bar{\nu}_\mu$ is RH (chirality). The muon is as discussed above



8 Weak interactions of leptons

- Coupling to all three generations is the same (can be verified by measuring at leptonic decays of taus)

8.1 Neutrino scattering

- Can generate beam of $\nu_\mu, \bar{\nu}_\mu$ by pointing a proton beam at a target and then using a magnet to select π^- or π^+
- Mass difference boosts neutrinos along pion direction
- Neutrino beam then hits a nucleon target
 - Q^2 is limited above by $Q^2 \leq 2m_N E_\nu$
 - $s \approx 2m_N E_\nu$
 - High-energy neutrino beams typically have $E_\nu = 200 - 400$ GeV

8.1.1 Nucleon cross-sections

- Angular dependence of cross-sections:

$$\begin{aligned} \frac{d}{d\Omega} \sigma_{\nu q}, \sigma_{\bar{\nu} \bar{q}} &\sim 1 \\ \frac{d}{d\Omega} \sigma_{\nu \bar{q}}, \sigma_{\bar{\nu} q} &\sim (1 + \cos \theta)^2 \end{aligned} \quad (74)$$

- The ν -X interaction cross-section is always $\sigma \propto s \approx 2m_X E_\nu$ (where the last approximation is in the limit $m_X \ll E_\nu$ and the target is at rest)
- At $E_\nu = 1$ GeV, $\sigma \sim 10$ fb
- $\sigma_{\nu q}/\sigma_{\bar{\nu} q} = 3$ (from integrating the angular dependence)
- Note $1 - y = \frac{1}{2}(1 + \cos \theta)$

8.1.2 Neutrino DIS

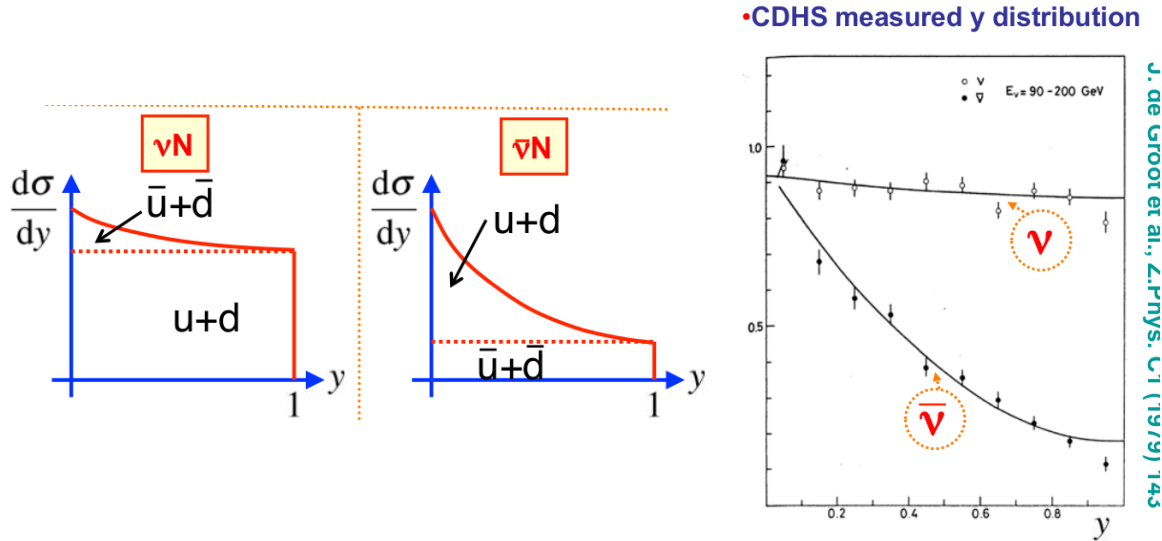
- First, define the quark/antiquark PDFs:

$$f_q = \int_0^1 dx \ x[u(x) + d(x)], \quad f_{\bar{q}} = \int_0^1 dx \ x[\bar{u}(x) + \bar{d}(x)] \quad (75)$$

- Then, the total neutrino-nucleon cross-sections are:

$$\begin{aligned} \frac{d\sigma_{\nu N}}{dy} &\propto E_\nu \left[f_q + (1 - y^2) f_{\bar{q}} \right] \\ \frac{d\sigma_{\bar{\nu} N}}{dy} &\propto E_\nu \left[(1 - y^2) f_q + f_{\bar{q}} \right] \end{aligned} \quad (76)$$

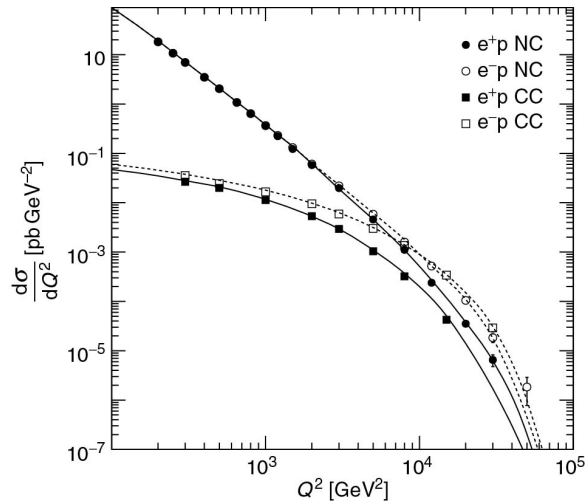
- Because $f_q \sim 5f_{\bar{q}}$ in a nucleon, we expect a shape difference in the cross-section
- First charged current neutrino DIS was at CDHS
 - ν_μ beam at scintillator/drift chamber detector.
 - Experimental signature is muon track and a large energy deposition in small area (from hadrons)



- First neutral current interactions were at Gargamelle
 - Also a ν_μ beam at a bubble chamber detector
 - Both nucleon DIS and electron scattering were looked for (hadronic shower and free e^- , respectively)
 - Reject events with final-state $\mu \Rightarrow$ cannot be weak current

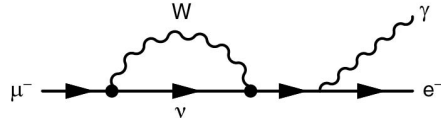
8.1.3 Weak contributions to e^-p scattering

- At high Q^2 , CC scattering starts to be comparable to (or even dominate) NC (since $\alpha_W > \alpha$)
 - Can be differentiated due to different final state: no final state lepton in CC
- In general, e^-p scattering cross-section is higher than e^+p scattering for two reasons:
 - CC: e^-p scattering probes high x part of u_V pdf, while e^+p probes d_V pdf (and $u_V(x) > d_V(x)$)
 - * At low Q^2 this difference can be ignored and sea antiquark pdfs become significant
 - NC: there is γ/Z interference at high Q^2 which is constructive for e^-p and destructive for e^+p



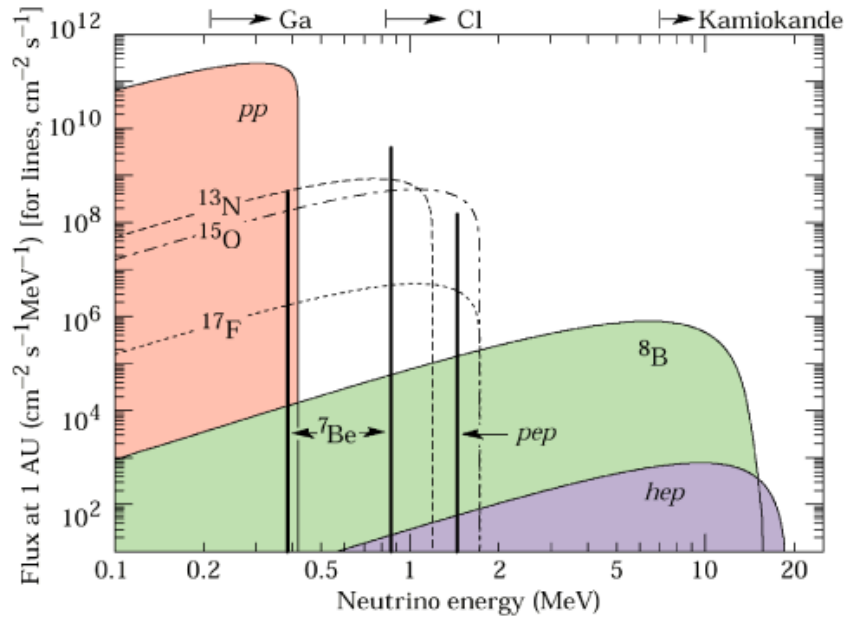
9 Neutrinos and oscillations

- We know that there are different flavors of neutrinos by searching for:



- Experiment puts $\text{Br}(\mu \rightarrow e^- \gamma) < 10^{-11}$

9.1 Solar neutrinos



- Main source of ν_e

- pp reactions:



- Binding energy of deuteron is only 2.2 MeV $\Rightarrow E_\nu < 0.5$ MeV
- Difficult to detect ($\sigma_{\nu N} \propto E_\nu$) so not used in experiments
- β -decay of ${}^8\text{B}$



- Most used in experiments
- E_ν up to 15 MeV

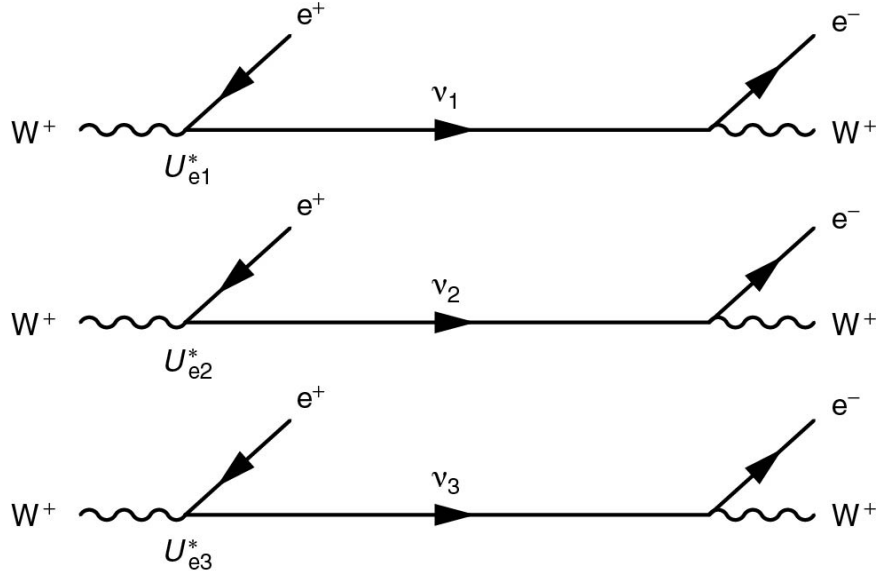
- Electron capture: ${}^7\text{Be} + e^- \rightarrow {}^7\text{Li} + \nu_e$
 - Two lines (corresponding to different electron excitations)
 - Two discrete lines $< 1 \text{ MeV}$
- $p + e^- + p \rightarrow {}^2\text{H} + \nu_e$
 - Single line at 1.5 MeV

9.1.1 Experimental detection

- Homestake
 - Large vat of C_2Cl_4
 - Flux was measured by counting number of ${}^{37}\text{Ar}$ atoms
 - $\nu_e + \text{Cl} \rightarrow \text{Ar} + e^-$
 - Found the solar neutrino problem
 - * Expected was 1.7 interactions per day
 - * Found .5 interactions per day
- Super-Kamiokande
 - 50 kt water Cerenkov detector surrounded by 11k PMTs
 - Counts $\nu_e e^- \rightarrow \nu_e e^-$ events (two leading-order t -channel diagrams involving W and Z)
 - * Stability of oxygen nucleus limits CC interaction with oxygen nucleons at low (solar neutrino) energies
 - Signature is ring of light
 - * e^- is stopped in chamber, so $N_\gamma \propto E_e$
 - * Can discriminate muons (from atmospheric neutrinos) due to sharper ring (e^- diffuse more). Muons only arise from NC interactions
 - Below $E_\nu < 5 \text{ MeV}$, radioisotope β -decay backgrounds dominate
 - Confirms solar neutrino deficit $\sim 1/2$ of expected flux
- SNO
 - Designed to detect electron neutrinos as well as total neutrino flux
 - Charged current
 - * $\nu_e + D(pn) \rightarrow e^- + p + p$
 - * $\nu_e + e^- \rightarrow \nu_e + e^-$ (also a NC diagram for this)
 - * Only ν_e participates because neutrino energies are not high enough to produce μ, τ
 - Neutral current
 - * $\nu_\ell + D(pn) \rightarrow \nu_\ell + p + n$
 - * $\nu_\ell + e^- \rightarrow \nu_\ell + e^-$
 - * All three flavors participate
 - Can measure total flux using all processes. Nucleon scattering has higher cross-sections
 - * Use elastic scattering off electrons to determine fraction of flux that comes from the sun (e^- direction is correlated with ν direction)
 - Results
 - * Again, confirms solar neutrino deficit
 - * On the other hand, found that the *total* neutrino flux from the Sun is equal to predicted ν_e flux \Rightarrow first indication of oscillations

9.2 Mass and weak eigenstates

- No reason to expect mass and weak eigenstates of neutrinos to be the same
- Mass eigenstates are the physical particle states
 - i.e. satisfy $i\partial_t \nu_k = E\nu_k$ for $k = 1, 2, 3$
- So a Feynman diagram with an internal ν_ℓ line is really the coherent addition of three diagrams with internal ν_k lines. If $k = 1, 2, 3$:



- Can define the ν_ℓ states as linear combinations of the particle states:

$$|\nu_\ell\rangle = \sum_{k=1,2,3} U_{\ell k}^* |\nu_k\rangle \quad (79)$$

- The W interaction vertex consequently must be written in terms of the mass eigenstates:

$$\left(-i U_{\ell k} \frac{g_W}{\sqrt{2}} \right) \bar{\ell} \gamma^\mu \frac{1}{2} (1 - \gamma^5) \nu_k \quad (80)$$

- For interactions involving an outgoing ν or incoming $\bar{\nu}$, U^* is in the vertex factor (i.e. the spinor is in the adjoint rep)
- If there is an incoming ν or outgoing $\bar{\nu}$, the spinor is in the fund. rep and U is used

9.2.1 Example: oscillation between two flavors

Here is the full derivation for oscillation between two flavors. Suppose there are two flavors e, μ and two mass eigenstates 1, 2. The free-particle states of the latter propagate as:

$$|\nu_k(t)\rangle = |\nu_k\rangle e^{-ip_k \cdot x} \quad (81)$$

where $p_k = (E_k, \mathbf{p}_k)$. Let us parametrize U by an angle θ :

$$\begin{pmatrix} \nu_e \\ \nu_\mu \end{pmatrix} = \begin{pmatrix} \cos \theta & \sin \theta \\ -\sin \theta & \cos \theta \end{pmatrix} \begin{pmatrix} \nu_1 \\ \nu_2 \end{pmatrix} \quad (82)$$

Suppose ν_e is produced at $t = 0$:

$$|\nu(0)\rangle = |\nu_e\rangle = \cos\theta|\nu_1\rangle + \sin\theta|\nu_2\rangle \quad (83)$$

The evolution is then given by the free particle equation above:

$$|\nu(x)\rangle = \cos\theta|\nu_1\rangle e^{-ip_1 \cdot x} + \sin\theta|\nu_2\rangle e^{-ip_2 \cdot x} \quad (84)$$

Now suppose the neutrino interacts weakly at a distance L and time T . It will be projected into a weak eigenstate. At this point, the wavefunction is:

$$|\nu(T, L)\rangle = \cos\theta|\nu_1\rangle e^{-i\phi_1} + \sin\theta|\nu_2\rangle e^{-i\phi_2}, \quad \phi_k = E_k T - p_k L \quad (85)$$

If we invert U and plug into the above equation:

$$\begin{aligned} |\nu(T, L)\rangle &= \cos\theta e^{-i\phi_1} [\cos\theta|\nu_e\rangle - \sin\theta|\nu_\mu\rangle] + \sin\theta e^{-i\phi_2} [\sin\theta|\nu_e\rangle + \cos\theta|\nu_\mu\rangle] \\ &= e^{-i\phi_1} \left(\left[\cos^2\theta + e^{i\Delta\phi_{12}} \sin^2\theta \right] |\nu_e\rangle + \left[1 - e^{i\Delta\phi_{12}} \right] \sin\theta \cos\theta |\nu_\mu\rangle \right) \end{aligned} \quad (86)$$

where

$$\Delta\phi_{12} = \phi_1 - \phi_2 \quad (87)$$

If $\Delta\phi_{12} \neq 0$, the ν_μ projection is non-zero. Squaring the factor multiplying $|\nu_\mu\rangle$, we get:

$$P(\nu_e \rightarrow \nu_\mu) = \sin^2(2\theta) \sin^2\left(\frac{\Delta\phi_{12}}{2}\right) \quad (88)$$

There are different assumptions one could make in calculating $\Delta\phi_{12}$ (in principle, one should evolve wavepackets instead of free particles). Here we assume $p_1 = p_2$, but one could also assume $E_1 = E_2$ or $\beta_1 = \beta_2$ and get the same answer.

$$\begin{aligned} \Delta\phi_{12} &= (E_1 - E_2)T - (p - p)L = \left[\sqrt{p^2 + m_1^2} - \sqrt{p^2 + m_2^2} \right] T \\ &\approx \left[p \left(1 + \frac{m_1^2}{2p^2} \right) - p \left(1 + \frac{m_2^2}{2p^2} \right) \right] T \\ &= (m_1^2 - m_2^2) \frac{L}{2p} \equiv \Delta m_{12}^2 \frac{L}{2E_\nu} \end{aligned} \quad (89)$$

In the last line, we assume $\beta \approx 1$ and $p \approx E_\nu$.

9.2.2 Oscillation between three flavors

- The calculation is similar to above, but more complicated
 - Have to deal with the fact that things like $e \rightarrow \mu \rightarrow \tau$ can happen, affecting the oscillation probabilities
- The matrix is known as the PMNS matrix
- The phase differences are defined as:

$$\Delta_{ij} = (m_i^2 - m_j^2) \frac{L}{4E_\nu} \equiv \Delta m_{ij}^2 \frac{L}{4E_\nu} \quad (90)$$

Note that they are not all independent. We can write $\Delta_{31} = \Delta_{32} + \Delta_{21}$

- The survival probability is:

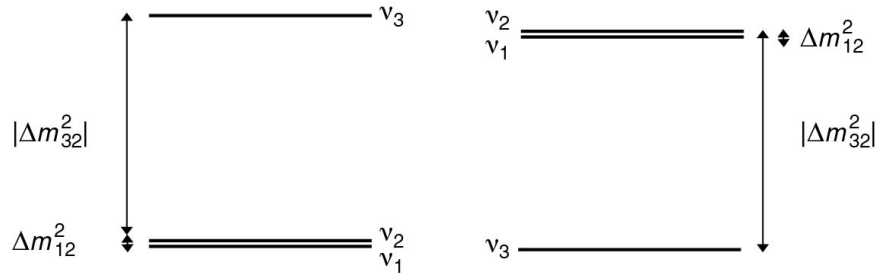
$$P(\nu_e \rightarrow \nu_e) = 1 - 4|U_{e1}|^2|U_{e2}|^2 \sin^2 \Delta_{21} - 4|U_{e1}|^2|U_{e3}|^2 \sin^2 \Delta_{31} - 4|U_{e2}|^2|U_{e3}|^2 \sin^2 \Delta_{32} \quad (91)$$

9.2.3 Neutrino masses

- Neutrino oscillation experiments are only sensitive to *difference* in squared masses, not the masses themselves
- Looking at end-point of electron Q distribution in tritium β -decay shows that the lightest eigenstate must be $\lesssim 2$ eV
- Large-scale structure and measurement of $C\nu B$ limit $\sum_k m_k \lesssim 1$ eV
- Best measurements of mass differences are:

$$\begin{aligned}\Delta m_{21}^2 &\sim 10^{-4} \text{ eV}^2 \\ \Delta m_{32}^2 &\sim 10^{-3} \text{ eV}^2\end{aligned}\quad (92)$$

- The sign of Δm_{32}^2 is unknown. $m_3 > m_2$ is the normal hierarchy; the inverse is the inverted hierarchy.



- Δm_{31}^2 has not been measured independently.

9.2.4 CP violation

- Recall that QED and QCD conserve C and P separately, so they cannot lead to CP violation. Weak interactions could be a source of CP violation.
- Two ways of determining if CP violation occurs in the PMNS matrix:
 - Measure $P(\nu_e \rightarrow \nu_\mu)$ and the CP -transformed quantity $P(\bar{\nu}_e \rightarrow \bar{\nu}_\mu)$ (note C is not enough since you would go from LH ν s to RH $\bar{\nu}$ s). Measure the difference in the probabilities; it should be 0 if CP is not violated
 - Assuming CPT invariance, CP violation implies T violation. Therefore, one could measure $P(\nu_\mu \rightarrow \nu_e)$ and check it is equal to $P(\nu_e \rightarrow \nu_\mu)$
- In order for this to occur, elements of the PMNS matrix must have imaginary components. There is in fact only one independent complex phase in the matrix (the others can be absorbed into particle definitions):

$$\begin{pmatrix} U_{e1} & U_{e2} & U_{e3} \\ U_{\mu 1} & U_{\mu 2} & U_{\mu 3} \\ U_{\tau 1} & U_{\tau 2} & U_{\tau 3} \end{pmatrix} = \begin{pmatrix} c_{12}c_{13} & s_{12}s_{13} & s_{13}e^{-i\delta} \\ -s_{12}c_{23} - c_{12}s_{23}s_{13}e^{i\delta} & c_{12}c_{23} - s_{12}s_{23}s_{13}e^{i\delta} & s_{23}c_{13} \\ -s_{12}s_{23} - c_{12}c_{23}s_{13}e^{i\delta} & c_{12}s_{23} - s_{12}c_{23}s_{13}e^{i\delta} & c_{23}c_{13} \end{pmatrix} \quad (93)$$

- Current experiments are not sensitive to CP violation in the neutrino sector

9.3 MSW effect

- In matter, the mass eigenstates are shifted slightly due to weak interactions with nucleons and electrons
 - The change in potential due to NC interactions with electrons and CC+NC interactions with nucleons is the same for all neutrino flavors

- However, the electron neutrino gets an additional CC interaction with electrons:

$$\Delta V(r) \equiv V_e(r) - V_{\mu,\tau}(r) = \sqrt{2}G_F N_e(r) \quad (94)$$

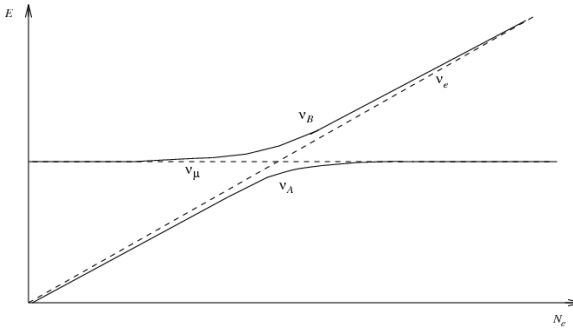
where $N_e(r)$ is the electron density as a function of position (i.e. r = distance from center of the Sun)

- The mixing due to this shift can become resonant if N_e is such that it satisfies:

$$A \equiv 2\sqrt{2}G_F N_e E_\nu = \Delta m_{21}^2 \cos(2\theta_{12}) \quad (95)$$

- “Resonance” refers to when the mixing is maximal, i.e. the mixing angle is 45°
- Note we are only considering $\nu_{1,2}$ because θ_{13} is very small

- If resonance is reached, $\nu_e a \approx \nu_2$ at the surface:



If this happens, then the probability of measuring ν_e at the Earth’s surface is $\sim \sin^2 \theta_{12}$. It is independent of L since the mass eigenstates don’t oscillate.

- If $E_\nu \geq 2$ MeV, then there is a point in the Sun where N_e satisfies the resonance condition
 - Note this is only possible if $\Delta m_{21}^2 \geq 0$. The fact that we observe this effect tells us the sign of the mass difference
 - We can try to measure $\text{sgn}(\Delta m_{32}^2)$ using atmospheric neutrinos through the Earth

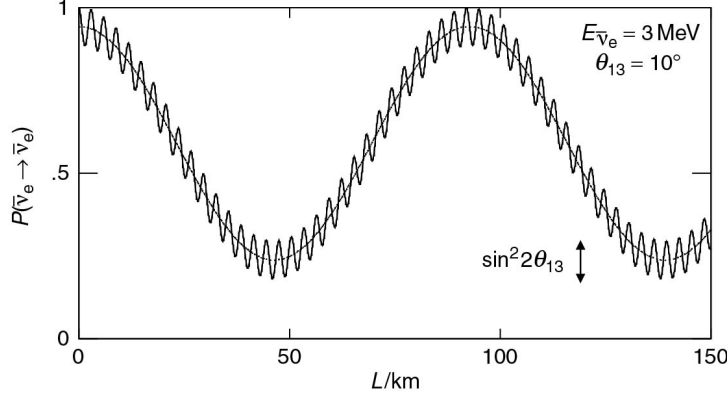
10 Oscillation experiments

- Both neutrinos and antineutrinos have t -channel CC and NC interactions with electrons and nucleons
 - Antineutrinos also have a s -channel CC interaction $\bar{\nu}_e e^- \rightarrow \bar{\nu}_e e^-$
- Muon neutrinos interact with electrons through CC only if $E_{\nu_\mu} > 11$ GeV (need to be able to create the muon). Threshold for taus is 3 TeV

10.1 Reactor experiments

- Use $\bar{\nu}_e$ flux from β^- decays of ^{235}U , ^{238}U , ^{239}Pu , ^{241}Pu
 - Flux is precisely known from power output of reactor
 - Energies are \sim MeV, so nucleon CC interaction is inverse β decay (as opposed to DIS)
- Because energies are too low to produce μ, τ in either nucleon or electron interactions, oscillation is observed through deficit of $\bar{\nu}_e$
- Two oscillation wavelengths

- Long-wavelength: sensitive to $\Delta m_{21}^2, \theta_{12}$. This is what solar neutrino experiments are sensitive to. $\mathcal{O}(100)$ km
- Short-wavelength: sensitive to $\Delta m_{32}^2, \theta_{13}$. $\mathcal{O}(1)$ km



10.1.1 Short baseline

- Sensitive to only short-wavelength oscillations

$$P(\bar{\nu}_e \rightarrow \bar{\nu}_e) \approx 1 - \sin^2(2\theta_{13}) \sin^2 \left(\frac{\Delta m_{32}^2 L}{4E_{\bar{\nu}}} \right) \quad (96)$$

- Daya Bay

- Detectors positioned at various distances from reactor cores (470, 580, 1650 m away)
- Detector is liquid scintillator loaded with Gd, surrounded by PMTs
- Inverse β -decay has highest cross-section ($\bar{\nu}_e + p \rightarrow e^+ + n$)
- Signal signature
 - * e^+ annihilates with an e^- and releases two prompt photons
 - * Low energy n drifts for a while until capture by a Gd nucleus, which then de-excites and releases a photon (timescale of 100 μs)
- Assuming known value of Δm_{32}^2 , Daya Bay measures:

$$\sin^2(2\theta_{13}) = 0.10 \pm 0.01 \quad (97)$$

- KamLAND

- Scintillator-PMT detector at 130-240 km away from reactor core
- Again, I β D is dominant process
- Signal signature
 - * Two prompt photons from e^+ annihilation
 - * Delayed 2.2 MeV photon from $n + p \rightarrow D + \gamma$
- Measured $\Delta m_{21}^2 \sim 8 \times 10^{-5} \text{ eV}^2$ and $\sin^2(2\theta_{12}) = 0.87$

10.1.2 Long baseline

- Relies on accelerator-based neutrino beams
- Use one near and one far detector. Systematic uncertainties will be the same, so can assume they cancel in the ratio when measuring survival probabilities
- MINOS
 - High intensity ν_μ beam from Fermilab
 - * $E_\nu \sim 1\text{-}5 \text{ GeV}$
 - * $L = 735 \text{ km}$
 - Dominant interaction is $\nu_\mu N \rightarrow \mu^- + \text{hadrons}$
 - Detector is planes of iron with plastic scintillator inbetween
 - * Magnetic field to curve charge particles
 - * Muon is identified and p_μ is measured by looking for a long curved track (hadrons will be stopped quickly)
 - * E_{had} is measured by amount of scintillation light near beginning of muon track (interaction vertex)
 - At these energies, the oscillation associated with Δ_{21} is much longer than L so can be ignored. Since θ_{13} is tiny, only μ, τ need to be considered
 - ν_τ energies are too low to produce a τ , so oscillation is measured by looking for a deficit of ν_μ interactions
 - Measures $|\Delta m_{32}^2| = 2.3 \times 10^{-3} \text{ eV}^2$ and $\sin^2(2\theta_{23}) \gtrsim 0.9$

10.2 Global picture

- Mass differences measured to within 5%:
 - $\Delta m_{21}^2 = 7.6 \times 10^{-5} \text{ eV}^2$
 - $\Delta m_{32}^2 = 2.3 \times 10^{-3} \text{ eV}^2$
- Three of the four PMNS parameters are measured (or are constrained):
 - $\sin^2(2\theta_{12}) = 0.87$
 - $\sin^2(2\theta_{23}) > 0.92$
 - $\sin^2(2\theta_{13}) = 0.10$
- The CP violating phase δ is not constrained at all
- Best measurement is:

$$\begin{pmatrix} \nu_e \\ \nu_\mu \\ \nu_\tau \end{pmatrix} = \begin{pmatrix} 0.82 & 0.54 & 0.15 \\ 0.35 & 0.70 & 0.62 \\ 0.44 & 0.45 & 0.77 \end{pmatrix} \begin{pmatrix} \nu_1 \\ \nu_2 \\ \nu_3 \end{pmatrix} \quad (98)$$

11 Weak interactions of quarks

11.1 CP violation and baryogenesis

- If there was no CP violation in the early universe, we would expect $n_B = n_{\bar{B}}$
 - Early universe was in thermal equilibrium with $\gamma + \gamma \leftrightarrow B + \bar{B}$ occurring at equal rates
 - As universe cooled and $k_B T < 2m_B$, the forward process stopped, freezing $n_B, n_{\bar{B}}$

- Experimentally, we measure:

$$\xi = \frac{n_B - n_{\bar{B}}}{n_\gamma} \approx \frac{n_B}{n_\gamma} \sim 10^{-9} \quad (99)$$

- Can be explained by very small asymmetry in early universe
 - For example, if $n_{\bar{B}} = 10^9$ and $n_B = 10^9 + 1$ in the early universe
 - If the baryons and antibaryons annihilated, today $n_{\bar{B}} = 0, n_B = 1, n_\gamma \sim 10^9$, giving the observed value of ξ

- Three conditions need to be met to make this mechanism work:
 - $A = n_B - n_{\bar{B}}$ is not constant
 - C and CP must be violated. If CP is conserved and there is a process that increases A , there would be a CP conjugate process decreasing it
 - Lack of thermal equilibrium. If the universe remained at thermal equilibrium, then any process that increases A would be canceled by the reverse process

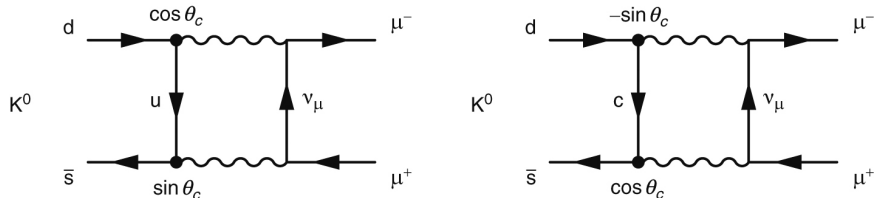
11.2 Cabibbo mixing and the weak interaction

- Let us start by assuming that the coupling of the weak interaction to *quark weak eigenstates* is universal. It turns out this is in agreement with observation
- Consider for now that there are only two generators of quarks
- As is the case for neutrinos, the down-type quark weak eigenstates are not the same as the mass eigenstates. Let q' be the weak eigenstates. Then:

$$\begin{pmatrix} d' \\ s' \end{pmatrix} = \begin{pmatrix} \cos \theta_C & \sin \theta_C \\ -\sin \theta_C & \cos \theta_C \end{pmatrix} \begin{pmatrix} d \\ s \end{pmatrix} \quad (100)$$

where $\theta_C \approx 13^\circ$ is the Cabibbo angle ($\cos \theta_C \approx 0.97$)

- The weak interaction vertices are modified accordingly. For example, the vertex factor for $W^+ \rightarrow \bar{d}c$ is $-\frac{g_W}{\sqrt{2}} \sin \theta_C$ (note \bar{d} refers to the *mass* eigenstate and $-\sin \theta_C$ is the overlap between d and s')
- The exact value of $\cos \theta_C$ can be extracted from the rate of nuclear β decay, for example
- Kaon decay and GIM mechanism



- Consider the decay $K_L \rightarrow \mu^+ \mu^-$. It can proceed through the box diagram on the left in the figure above. The matrix element is proportional to:

$$\mathcal{M} \propto g_W^4 \cos \theta_C \sin \theta_C \quad (101)$$

- However, the observed BR is much *smaller* than would be expected from this one diagram. When this was observed, the c quark had not been discovered.

- However, if we include the c quark and use the Cabibbo mixing matrix, then we get the diagram on the right. The matrix element is:

$$\mathcal{M} \propto -g_W^4 \cos \theta_C \sin \theta_C \quad (102)$$

Note the minus sign is from the d, s' element of the matrix

- Adding these matrix elements leads to a cancellation. The cancellation is not exact because the matrix element includes kinematic factors (which are slightly different for a virtual u and c)

11.3 The CKM matrix

- We can extend the above argument to three generations using the CKM matrix:

$$\begin{pmatrix} d' \\ s' \\ b' \end{pmatrix} = \begin{pmatrix} V_{ud} & V_{us} & V_{ub} \\ V_{cd} & V_{cs} & V_{cb} \\ V_{td} & V_{ts} & V_{tb} \end{pmatrix} \begin{pmatrix} d \\ s \\ b \end{pmatrix} \quad (103)$$

- Vertex factors are modified accordingly. If the up-type quark is leaving the interaction, use V ; otherwise use V^*
- Like the PMNS matrix, the CKM matrix is parametrized by three angles ($\phi_{12}, \phi_{23}, \phi_{13}$) and a phase shift (δ')
- The magnitude of each element of V can be measured independently:

- V_{ud} : superallowed $0^+ \rightarrow 0^+$ nuclear β decays
- V_{us} : decay rate of $K_L^0(d\bar{s}) \rightarrow \pi^-(d\bar{u}) + e^+\nu_e$
- V_{ub} : decay rate of $B^0(d\bar{b}) \rightarrow \pi^-(d\bar{u}) + e^+\nu_e$
- V_{cd} : cross-section of $\nu_\mu d \rightarrow \mu^- c$, where the c is identified by its decay to $s\mu^+\nu_\mu$.
- V_{cs} : decay rate of $D_s^+(c\bar{s}) \rightarrow \mu^+\nu_\mu$
- V_{cb} : decay rate of B mesons to final states with charm
- V_{td} and V_{ts} : oscillation rate of $B^0 \leftrightarrow \bar{B}^0$
- V_{tb} : decay rate of $t \rightarrow bW$ (large uncertainties)

- The observed magnitudes are:

$$|V| = \begin{pmatrix} 0.974 & 0.225 & 0.004 \\ 0.225 & 0.973 & 0.041 \\ 0.009 & 0.040 & 0.999 \end{pmatrix} \quad (104)$$

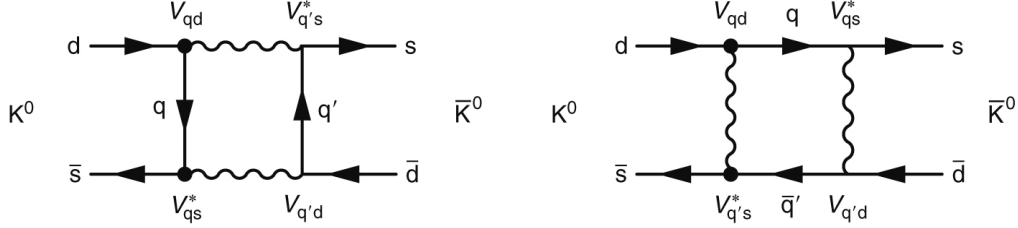
11.4 Neutral kaon system

- Neutral kaons ($d\bar{s}$ and $s\bar{d}$) can be produced strongly:

$$\begin{aligned} \pi^-(d\bar{u}) + p(uud) &\rightarrow \Lambda(uds) + K^0(d\bar{s}) \\ p(uud) + \bar{p}(\bar{u}\bar{u}\bar{d}) &\rightarrow K^+(u\bar{s}) + \bar{K}^0(s\bar{d}) + \pi^-(d\bar{u}) \end{aligned} \quad (105)$$

Thus, K^0, \bar{K}^0 are strong (flavor) eigenstates

- Neutral kaons are the lightest charmed bound states, so they must decay weakly.
 - For mass reasons, the decay must be leptonically or to pions
 - Neutral kaons can also mix with each other:



- Therefore, the physical states are not K^0, \bar{K}^0 : if a K^0 is produced, it will not stay a K^0 . Physical states only evolve through phase rotations
- The real physical states are linear combinations of K^0, \bar{K}^0 . Call them K_S, K_L . It turns out their masses are quite close (~ 498 MeV), but their lifetimes are quite different:

$$\tau_{K_S} \sim 10^{-10} \text{ s} < \tau_{K_L} \sim 10^{-7} \text{ s} \quad (106)$$

11.4.1 Kaon CP eigenstates

- On the road to constructing K_S, K_L , let us first figure out the CP eigenstates of the system
- The action of CP is:

$$CP \begin{pmatrix} K^0 \\ \bar{K}^0 \end{pmatrix} = \begin{pmatrix} \bar{K}^0 \\ K^0 \end{pmatrix} \quad (107)$$

implying that the CP eigenstates are:

$$K_1 = \frac{K^0 + \bar{K}^0}{\sqrt{2}}, \quad K_2 = \frac{K^0 - \bar{K}^0}{\sqrt{2}} \quad (108)$$

- The CP of K_1 (K_2) is $+1$ (-1)
- If CP were conserved, K_S, K_L would be the same as K_1, K_2 . However, due to a weak CP violation, this equality is close but not exact

11.4.2 Kaon decays to pions

- It is observed that K_S decays to two neutral pions much faster than it decays to three neutral pions; the converse is true for K_L
- $K_{S,L} \rightarrow \pi^0 \pi^0$ or $\pi^+ \pi^-$
 - Since neutral kaons and pions are $J^P = 0^-$, the angular momentum of the final state must be $l = 0$
 - $\Rightarrow CP$ of the final state is $+1$ (true for either final state)
- $K_{S,L} \rightarrow \pi^0 \pi^0 \pi^0$ or $\pi^+ \pi^- \pi^0$
 - Similar arguments can be made to show the final state is $CP = -1$
- If CP were conserved (which it almost is):
 - The only way to get to the two-pion (CP -even) final state is to start with K_1
 - The only way to get to the three-pion (CP -odd) final state is to start with K_2
- The decay to two pions is obviously favored for mass reasons, so K_1 decays much faster than K_2

$$m_K - 2m_\pi = 220 \text{ MeV} > m_K - 3m_\pi = 80 \text{ MeV} \quad (109)$$

- Because CP is slightly violated, the decays $K_L \rightarrow \pi\pi$ and $K_S \rightarrow \pi\pi\pi$ are not forbidden, just very suppressed

11.4.3 CP violation in kaons

- Can be detected in the following way (à la Cronin and Fitch):
 - Start with a beam of pure K^0 (or \bar{K}^0). Can be achieved in $p\bar{p}$ collisions as described above
 - Allow the beam to travel for a distance $L \gg c\tau_S$, so that all the K_S have decayed
 - Look for two-pion decays in the remaining beam of K_L
 - Found to be $\sim 0.3\%$ (inclusive)
- Two ways of introducing CP violation: in the mixing of $K^0 \leftrightarrow \bar{K}^0$ or in the decay of the CP eigenstate itself
- CP violation in kaon mixing
 - This turns out to be the dominant effect and is due to CP violation in the CKM matrix
 - The mass eigenstates are:
$$K_S = \frac{K_1 + \varepsilon K_2}{\sqrt{1 + |\varepsilon|^2}}, \quad K_L = \frac{\varepsilon K_1 + K_2}{\sqrt{1 + |\varepsilon|^2}} \quad (110)$$

for a small complex parameter ε
- CP violation in kaon decay
 - Also due to CP -violating phase in CKM matrix
 - Parametrized by ε' . NA48 and KTeV measure:
$$\Re \frac{\varepsilon'}{\varepsilon} \sim 10^{-3} \quad (111)$$

11.5 Kaon oscillation

- Suppose we produce a beam of K^0 . As noted above, it mixes with \bar{K}^0 (or equivalently, the K_L, K_S components of the wavefunction evolve separately)
- Let us assume for now that CP is conserved (violation has a small effect on the oscillation)
- Like neutrinos, we can compute the probabilities $P(K^0 \rightarrow K^0), P(K^0 \rightarrow \bar{K}^0)$

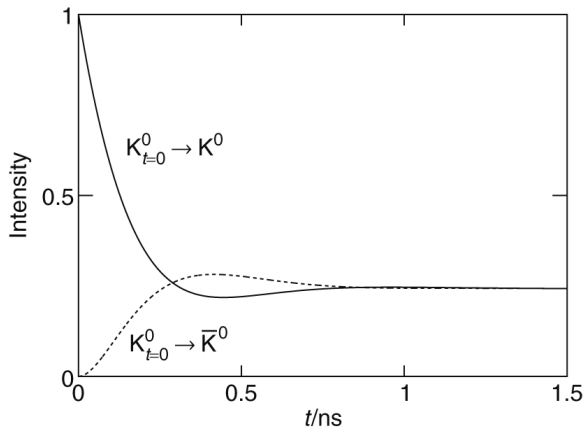
$$\begin{aligned} P(t; K^0 \rightarrow K^0) &\propto e^{-\Gamma_S t} + e^{-\Gamma_L t} + 2e^{-\frac{1}{2}(\Gamma_S + \Gamma_L)t} \cos(t\Delta m) \\ P(t; K^0 \rightarrow \bar{K}^0) &\propto e^{-\Gamma_S t} + e^{-\Gamma_L t} - 2e^{-\frac{1}{2}(\Gamma_S + \Gamma_L)t} \cos(t\Delta m) \end{aligned} \quad (112)$$

The above equations neglect CP violation (a small effect)

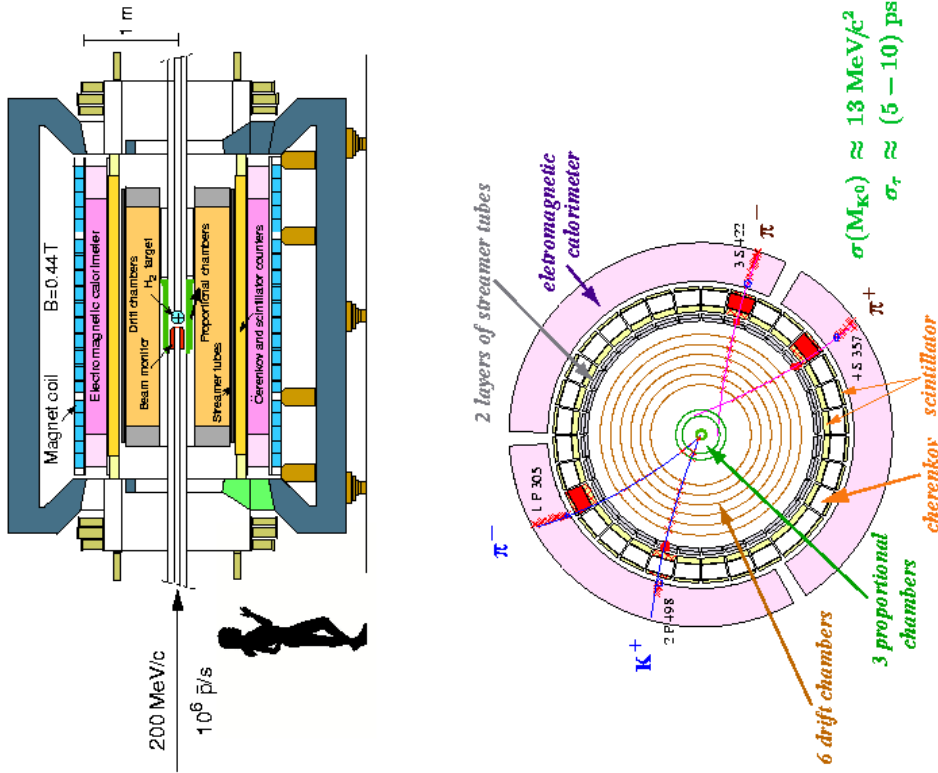
- Unlike neutrinos, these probabilities are *not* sinusoidal and do not have to add to one
- This is because the kaon may decay
- The difference in widths Γ_L, Γ_S is due to interference arising from decays of K^0 and \bar{K}^0 to the same final state
 - Details in Thomson, equations 14.23 and 14.31
- We find (experimentally, described below) that:

$$T_{\text{osc}} = \frac{2\pi\hbar}{\Delta m} \sim 10^{-9} \text{ s}, \quad \Delta m = m_{K_L} - m_{K_S} \quad (113)$$

which is one order of magnitude greater than τ_{K_S} . Therefore, the K_S component decays out before one oscillation is even completed, leaving a pure K_L beam. Note that the intensity of K^0 and \bar{K}^0 is the same at this point, since $|\langle K^0 | K_L \rangle|^2 = |\langle \bar{K}^0 | K_L \rangle|^2$ (assuming no CP violation):



11.5.1 CPLEAR detector



- Beam of antiprotons with momentum 200 MeV is aimed at a gaseous hydrogen target
- We go through the detector components, from inside to outside:
 - 2 concentric cylindrical MWPCs
 - Used for tracking and triggering on tracks from primary interaction or kaon decay
 - Drift gas has composition close to magic gas
 - Radii are 10 cm and 13 cm
 - 6 concentric cylindrical drift chambers

- Main tracking detectors
- Momentum resolution is 5%
- Drift gas is half-and-half ethane and argon
- Two streamer tubes
 - Immediately outside drift chambers
 - Used to provide z -position measurement quickly online
- Particle ID detectors
 - Consists of 32 sectors: Cerenkov detector sandwiched between two layers of scintillators

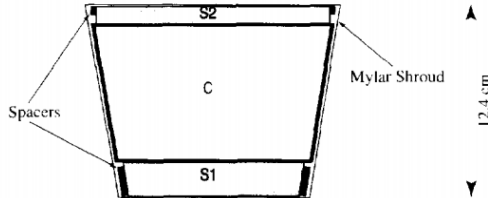


Fig. 25. Cross section of one of the 32 PID sectors (S1, S2: scintillators, C: Cerenkov detector).

- Light collection is done by PMTs (different channels for the three components)
- Inner scintillator is 3 cm and outer is 1.4 cm. Both are plastic
- Cerenkov detector is 8 cm thick
- Cerenkov light threshold is $\beta > 0.84 \Rightarrow$ non-relativistic kaons do not produce a signal

11.5.2 Experimental discovery of neutral kaon oscillation

- CPLEAR used $p\bar{p}$ collisions to produce $K^-\pi^+K^0$ and $K^+\pi^-\bar{K}^0$
 - Can use the charge of the charged kaon and pion to determine the state of the neutral kaon when it was produced
 - * K^\pm is distinguished from π^\mp because the π will be relativistic \Rightarrow leaves signal in Cerenkov detector
 - Since the leptonic decays are $K^0 \rightarrow \pi^-\ell^-\bar{\nu}_\ell$ and $\bar{K}^0 \rightarrow \pi^+\ell^+\nu_\ell$, the charge of the lepton can be used to identify the state of the neutral kaon when it decayed
- COM energy low enough that the kaons are produced close to rest
 - Low velocity \Rightarrow oscillation and decay can occur within the detector
- In the neutral kaon $\rightarrow \pi\ell\nu$ decay, the charged pion and lepton leave curved tracks in the tracker
 - Can find vertex of tracks to determine where the neutral kaon decayed
 - Distance from interaction point is the distance traveled L
- Provides an experimental way of measuring the probabilities:

$$\begin{aligned} P(t; K^0 \rightarrow K^0), \quad P(t; K^0 \rightarrow \bar{K}^0) \\ P(t; \bar{K}^0 \rightarrow \bar{K}^0), \quad P(t; \bar{K}^0 \rightarrow K^0) \end{aligned} \quad (114)$$

where we have switched from L to t

- Can extract the difference in mass eigenstates from the oscillation period, finding $\Delta m \sim 10^{-15}$ GeV

11.5.3 Measurement of CP violation

- ε (the CP violation parameter in the neutral kaon system) was extracted by CPLEAR by measuring the asymmetry:

$$A_{+-} = \frac{\Gamma(\bar{K}^0 \rightarrow \pi^+ \pi^-) - \Gamma(K^0 \rightarrow \pi^+ \pi^-)}{\Gamma(\bar{K}^0 \rightarrow \pi^+ \pi^-) + \Gamma(K^0 \rightarrow \pi^+ \pi^-)} \quad (115)$$

finding:

$$\varepsilon = |\varepsilon| e^{i\phi}, \quad \varepsilon = 2.3 \times 10^{-3}, \quad \phi = 43^\circ \quad (116)$$

- Can also look at semileptonic decays of K_L to measure ε :

$$\delta = \frac{\Gamma(K_L \rightarrow \pi^- e^+ \nu_e) - \Gamma(K_L \rightarrow \pi^+ e^- \bar{\nu}_e)}{\Gamma(K_L \rightarrow \pi^- e^+ \nu_e) + \Gamma(K_L \rightarrow \pi^+ e^- \bar{\nu}_e)} \approx 2|\varepsilon| \cos \phi \quad (117)$$

A beam of pure K_L is achieved by simply waiting $t \gg \tau_S$

11.6 B -meson physics

- Neutral meson oscillation also occurs for:

$$B^0(d\bar{b}) \leftrightarrow \bar{B}^0(b\bar{d}), \quad B_s^0(s\bar{b}) \leftrightarrow \bar{B}_s^0(b\bar{s}), \quad D^0(u\bar{c}) \leftrightarrow \bar{D}^0(c\bar{u}) \quad (118)$$

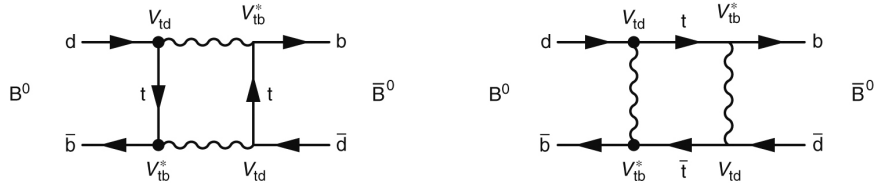
- Here we consider B^0 oscillation

- Can carry out a similar calculation what was done for kaons to find the physical states:

$$B_L = \frac{1}{\sqrt{2}} (B^0 + e^{-i2\beta} \bar{B}^0), \quad B_H = \frac{1}{\sqrt{2}} (B^0 - e^{-i2\beta} \bar{B}^0) \quad (119)$$

where β is the phase of V_{td} : $V_{td} = |V_{td}| e^{-i\beta}$.

- L, H refer to the lighter, heavier states
- In doing this calculation, only diagrams with virtual t are considered since $|V_{tb}| \gg |V_{ts}|, |V_{td}|$:

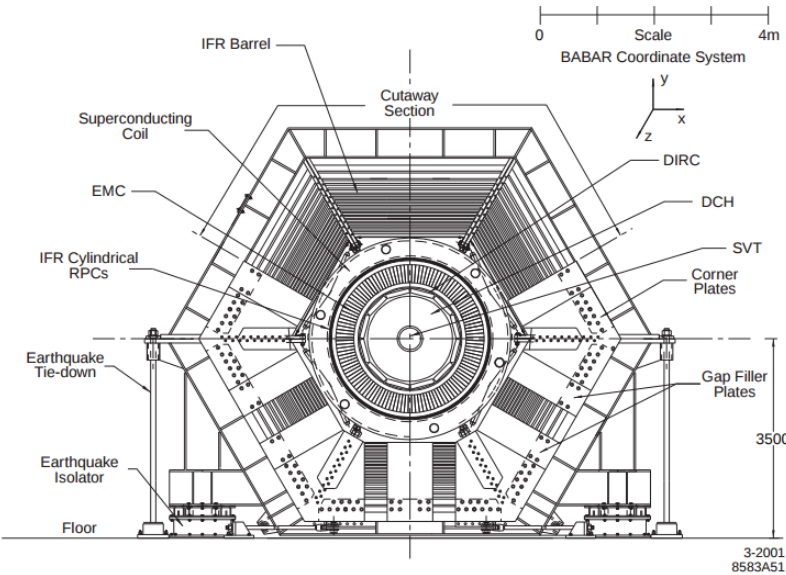


- The difference in the masses of the two states is $\Delta m_d \propto |(V_{td}V_{tb}^*)^2|$. The masses are ~ 5.3 GeV
- The lifetimes of the two states are very close ($\tau \sim 10^{-12}$ s)
 - * The lifetimes are close because there is negligible interference in the decays of B^0 and \bar{B}^0
- Note the lifetimes are much smaller than the kaon lifetimes because $m_B \gg m_K$, opening up the phase space for decays
- The probabilities of oscillation are computed in a similar way as done for kaons

$$\begin{aligned} P(t; B^0 \rightarrow B^0) &= e^{-\Gamma t} \cos^2 \left(\frac{\Delta m_d t}{2} \right) \\ P(t; B^0 \rightarrow \bar{B}^0) &= e^{-\Gamma t} \sin^2 \left(\frac{\Delta m_d t}{2} \right) \end{aligned} \quad (120)$$

- The results are a bit simpler since the two states have the same width
- Note, we ignored CP violation, as the effect is tiny

11.6.1 BaBar detector



- Going through the detector components, from inside to out:
 - Silicon vertex tracker
 - Used for tracking and position measurement
 - * Standalone tracking for particles with momentum < 120 MeV
 - 5 layers of double-sided Si strips
 - Vertex resolution along z -axis is < 80 μm . In x - y plane, it is $\sim 100 \mu\text{m}$
 - Extend from 32 to 144 mm
 - Drift chamber
 - Main tracking detector and can do PID through dE/dx
 - 40 layers of wires from 23.6 to 80.9 cm
 - Helium-based gas
 - Cerenkov detector
 - Detects Cerenkov photons that are trapped in the crystal due to total internal reflection. Photons travel the length of the detector to PMTs in endcap that are outside the \vec{B} -field
 - θ_C is preserved in total internal reflection
 - 1.7 cm thick detectors
 - Used to identify charged kaons, pions, and low-momentum muons (< 750 MeV)
 - * Done using the Cerenkov angles
 - EM calorimeter
 - Particle ID for e^- , γ , charged hadrons
 - Scintillator crystals of CsI; light output to PMTs
 - * Rad length is 1.85 cm
 - * Molière radius is 3.6 cm

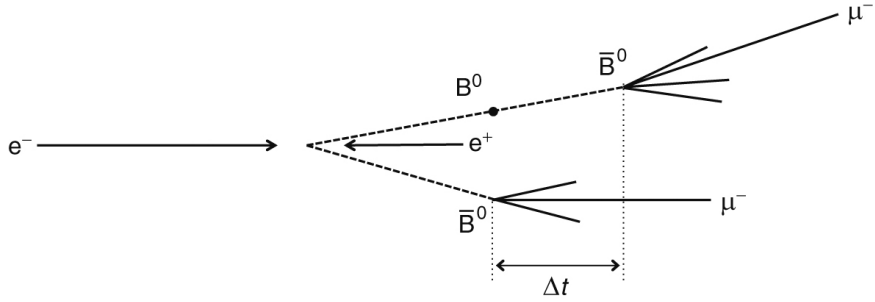
- * dE/dx for MIP is 5.6 MeV/cm
- * $\sim 4 \times 10^4$ photons per MeV
- * $\sigma_E/E \sim 1\%$
- Thickness is $\sim 15X_0$
- Solenoid
 - 1.5 T \vec{B} -field
- Instrumented flux return
 - Muon and neutral hadron ID
 - Also functions as magnet yoke for return field
 - Instrumented with resistive plate counters
 - Graded into 2-10 cm segments of iron
 - Active volume is filled with mostly argon and freon, with a small amount of isobutane

11.6.2 Experimental measurement of B^0 oscillation

- Belle and BaBar used e^-e^+ beams with $\sqrt{s} = 10.58$ GeV = $m_{\Upsilon(4S)}$.
- $\Upsilon(4S)$ is a $b\bar{b}$ resonance that decays to B^+B^- or $B^0\bar{B}^0$
 - Since $m_{\Upsilon(4S)} \sim 2m_B$, the B mesons are produced approximately at rest in the COM frame
- The lifetime of the neutral B meson ($\sim 10^{-12}$ s) is rather short, so to extend the distance traveled before decay, the beams are asymmetric
 - BaBar used $E_e^- = 9$ GeV and $E_e^+ = 3.1$ GeV
 - The $\beta\gamma$ of the $\Upsilon(4S)$ (or BB system) is $5.9/10.58 = 0.56$
 - Neutral B mesons therefore travel $\sim \mathcal{O}(100)$ μm before decaying
- Leptonic decays were used because the sign of the lepton charge tags the flavor of the B meson:

$$B^0(d\bar{b}) \rightarrow D^-(d\bar{c}) + \mu^+\nu_\mu, \quad \bar{B}^0(b\bar{d}) \rightarrow D^+(c\bar{d}) + \mu^-\bar{\nu}_\mu \quad (121)$$

- A typical neutral B -meson event at Belle or BaBar looks like:



- Here is what happens in an event:
 1. The $\Upsilon(4S)$ is produced and decays to $B^0\bar{B}^0$ system.

2. The $B^0\bar{B}^0$ system travels for a while as a coherent state. Until one of the B s decay, the mesons remain in a linear combination of the two flavor states
 3. One of the mesons decays into a final state containing a μ^- , therefore tagging it as \bar{B}^0 . Call this time $t = 0$. At $t = 0$, the other meson must be a pure B^0 state, since the one that decayed collapsed into the \bar{B}^0 state
 4. The B^0 then propagates, evolving as described previously. At some time $t = \Delta t$, a μ^- is detected, indicating that the B^0 has oscillated into a \bar{B}^0 and decayed
- By counting the number of such events as a function of the proper time $\Delta\tau = \Delta t/\gamma$, we get:

$$N(t + \delta t; B^0 \rightarrow \bar{B}^0) \quad (122)$$

Note we have changed nomenclature $\Delta\tau \rightarrow t$ in the above equation to be consistent with what was done before. δt is the binning used

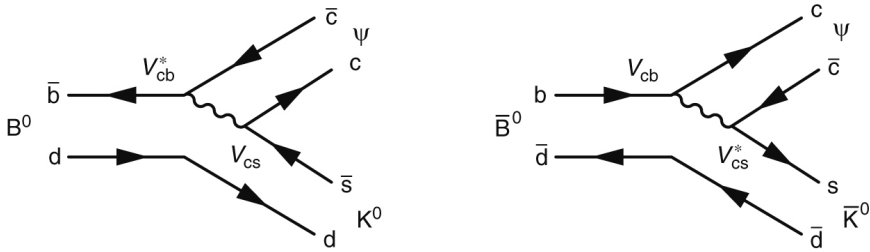
- By doing the same thing, except flipping the sign of one or both muons, we get the number of each type of oscillation
- By normalizing correctly, we get the oscillation probabilities. For example:

$$P(t; B^0 \rightarrow \bar{B}^0)\delta t = \frac{N(t + \delta t; B^0 \rightarrow \bar{B}^0)}{N(t + \delta t; B^0 \rightarrow B^0) + N(t + \delta t; B^0 \rightarrow \bar{B}^0)} \quad (123)$$

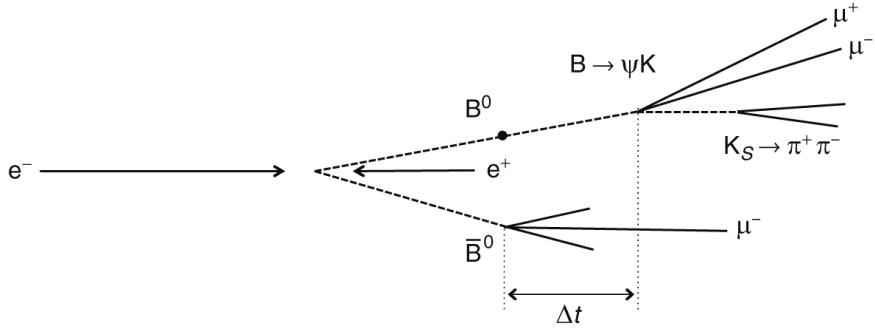
- Extracting this as a function of t allows us to extract Δm_d . Assuming $|V_{tb}| \sim 1$, we can extract $|V_{td}|$

11.6.3 CP violation in the neutral B system

- There are three ways to introduce CP violation in neutral B mesons:
 1. CP violation in the decay $\Gamma(A \rightarrow X) \neq \Gamma(\bar{A} \rightarrow \bar{X})$. This is what happens in $K^0 \rightarrow 2\pi, 3\pi$ vs $\bar{K}^0 \rightarrow 2\pi, 3\pi$
 2. CP violation in the mixing $B^0 \leftrightarrow \bar{B}^0$. This also happens for kaons
 3. CP violation in the interference between decays to a common final state, i.e. between $B^0 \rightarrow f$ and $B^0 \rightarrow \bar{B}^0 \rightarrow f$
- It turns out only (3) has a significant contribution for B mesons. In what follows, we omit all other sources of CP violation
- To isolate this effect, one can look at the $B \rightarrow J/\psi + K$ decay. In what follows, we label J/ψ simply as ψ . The Feynman diagrams for the decay are:



- $\psi(1^-)$ and $K_S(0^-)$ are both $CP = +1$. The final state must have $l = 1$, since the B mesons are 0^- . Therefore, $CP(\psi K_S) = -1$
- Belle and BaBar looked for the following decay:



As with the measurement of the oscillation probabilities, we can use the flavor of the first lepton to determine the flavor of the B mesons.

- Note that we know the kaon is K_S when it decays because K_L would not decay within the detector
- We can then calculate the asymmetry:

$$A_{CP}^{K_S} = \frac{\Gamma(\bar{B}^0 \rightarrow \psi K_S) - \Gamma(B^0 \rightarrow \psi K_S)}{\Gamma(\bar{B}^0 \rightarrow \psi K_S) + \Gamma(B^0 \rightarrow \psi K_S)} = \sin(t\Delta m_d) \sin(2\beta) \quad (124)$$

and directly extract β

12 Electroweak unification

12.1 W boson properties

- Since the W boson is a massive spin-1 boson, it has three polarizations (one longitudinal and two transverse)
- The partial width of the decay to leptons is:

$$\Gamma(W^- \rightarrow e^- \bar{\nu}_e) = \frac{g_W^2 m_W}{48\pi} \quad (125)$$

- The partial width to quarks must take into account the CKM matrix (discussed above):

$$\Gamma(W^+ \rightarrow q_u \bar{q}_d) = 3|V_{q_u q_d}|^2 \Gamma_{e \nu_e} \quad (126)$$

where q_u, q_d are up-, down-type quarks respectively. Note $t\bar{q}_d$ is forbidden for mass reasons. The factor of 3 accounts for multiple colors.

- The total width to quarks is:

$$\Gamma(W^+ \rightarrow q\bar{q}') = 6\Gamma_{e \nu_e} \quad (127)$$

since unitarity implies $\sum_{q_d} |V_{uq_d}|^2 = \sum_{q_d} |V_{cq_d}|^2 = 1$

- In principle, one can calculate the total width and branching fraction given this information:

$$\Gamma_W = (3 + 6) \times \Gamma_{e \nu_e}, \quad BR(W \rightarrow q\bar{q}') = \frac{6\Gamma_{e \nu_e}}{3\Gamma_{e \nu_e} + 6\Gamma_{e \nu_e}} \quad (128)$$

- However, care has to be taken to account for higher-order QCD processes, such as $W \rightarrow q\bar{q}'g$. The quark decay matrix elements are therefore multiplied by:

$$\kappa_{QCD} = 1 + \frac{\alpha_S(m_W)}{\pi} \approx 1.04 \quad (129)$$

which implies:

$$\Gamma_W = (3 + 6\kappa_{QCD}) \times \Gamma_{e \nu_e} = 2.1 \text{ GeV}, \quad BR(W \rightarrow q\bar{q}') = \frac{6\kappa_{QCD}}{3 + 6\kappa_{QCD}} = 0.675 \quad (130)$$

- Let us consider the process $e^-e^+ \rightarrow W^+W^-$. There is a t -channel diagram with an exchanged ν_e and an s -channel through a γ .
 - However, it is found that σ increases without bound as a function of s if only these two diagrams are considered (breaks unitarity eventually)
 - In particular, \mathcal{M}_ν increases and the destructive interference between \mathcal{M}_ν and \mathcal{M}_γ is not enough to cancel this increase
 - This can be fixed by adding an additional s -channel diagram through an additional (Z) boson

12.2 The gauge structure: $SU(2)_L$

- The weak interaction arises from an $SU(2)$ symmetry. Left-handed particles (right-handed antiparticles) are in doublet representations of this symmetry:

$$\mathbf{T} = \frac{1}{2}\boldsymbol{\sigma}, \quad \begin{pmatrix} \nu_{e,L} \\ e_L^- \end{pmatrix}, \quad \begin{pmatrix} u_L \\ d_L \end{pmatrix}, \quad \dots \quad (131)$$

The top/bottom members of these doublets have $I_W^{(3)} = \pm \frac{1}{2}$.

- Right-handed particles (left-handed anti-particles) are in singlet representations: $e_R^-, u_R, \bar{\nu}_{e,L}, \dots$. These all have $I_W^{(3)} = 0$.
- The three gauge fields corresponding to the three generators are $W_\mu^{(i)}$ (corresponding to T_i)
- The charged W bosons are linear combinations of two bosons:

$$W_\mu^\pm = \frac{1}{\sqrt{2}} (W_\mu^{(1)} \mp W_\mu^{(2)}) \quad (132)$$

and the corresponding currents are (using the example of the electron doublet):

$$j_\pm^\mu = \frac{g_W}{\sqrt{2}} (\bar{\nu}_e \quad \bar{e}) \gamma^\mu \frac{1}{2} (1 - \gamma^5) [T_1 \pm iT_2] \begin{pmatrix} \nu_e \\ e \end{pmatrix} \quad (133)$$

- We could identify the third gauge boson with the physical Z boson, but it is observed that the Z couples to both LH and RH chiral particles (but not equally). Therefore, the Z is a linear combination of $W^{(3)}$ and something else.

12.3 Electroweak unification

- We add an additional $U(1)_Y$ symmetry to the model, which couples to fermions:

$$\psi(x) \rightarrow \exp \left[ig' \frac{Y_\psi}{2} \alpha(x) \right] \psi(x) \quad (134)$$

where Y_ψ is the hypercharge of particle ψ . The corresponding gauge field is labeled B^μ

- We then define the physical Z and A fields as:

$$\begin{aligned} A_\mu &= B_\mu \cos \theta_W + W_\mu^{(3)} \sin \theta_W \\ Z_\mu &= -B_\mu \sin \theta_W + W_\mu^{(3)} \cos \theta_W \end{aligned} \quad (135)$$

where θ_W is the weak mixing angle.

- To reproduce the observed QED charges/couplings, the following constraints must hold:

$$e = g_W \sin \theta_W = g' \cos \theta_W, \quad Y = 2 \left(Q - I_W^{(3)} \right) \quad (136)$$

- The easiest way to measure the weak mixing angle is through $e^- e^+ \rightarrow Z \rightarrow f\bar{f}$, giving $\sin^2 \theta_W = 0.23$
- The vertex factor for the Z can be written in terms of couplings to the vector and axial components of the field:

$$-i \frac{g_Z}{2} \gamma^\mu \left[c_V - c_A \gamma^5 \right], \quad g_Z = \frac{g_W}{\cos \theta_W} \quad (137)$$

The values of c_V, c_A depend on the particle:

$$\begin{aligned} c_V &= I_W^{(3)} - 2Q \sin^2 \theta_W \\ c_A &= I_W^{(3)} \end{aligned} \quad (138)$$

- The partial width then is:

$$\Gamma(Z \rightarrow f\bar{f}) = \frac{g_Z^2 m_Z}{4\pi} \left(c_V^2 + c_A^2 \right) \Rightarrow \Gamma_Z \sim 2.5 \text{ GeV} \quad (139)$$

- The branching ratios are:

$$\begin{aligned} BR(Z \rightarrow \nu\bar{\nu}) &\sim 0.21 \\ BR(Z \rightarrow \ell\bar{\ell}) &\sim 0.1 \\ BR(Z \rightarrow \text{hadrons}) &\sim 0.69 \end{aligned} \quad (140)$$

12.4 Experimental measurements of electroweak theory

12.4.1 Discovery of W and Z bosons

- Done at SPS in $p\bar{p}$ collisions
- Invention of stochastic cooling as a way to reduce the p_\perp of particles in the beam. Done using \vec{E} -field pulses

12.4.2 Measurement of the Z peak

- Done at LEP, using $e^- e^+$ collisions, scanning \sqrt{s} near Z mass, allowing the resonance to be measured
- Because the Z has a finite lifetime, the propagator has to be modified:

$$\frac{1}{q^2 - m_Z^2} \rightarrow \frac{1}{q^2 - m_Z^2 + im_Z \Gamma_Z} \quad (141)$$

The cross-section still peaks at $\sqrt{s} = m_Z$ (for the s -channel diagram), but it is a peak of finite width Γ_Z :

$$\sigma \propto \frac{1}{(s - m_Z^2)^2 + (m_Z \Gamma_Z)^2} \quad (142)$$

- The cross-section of $e^- e^+ \rightarrow Z \rightarrow f\bar{f}$ can be written as:

$$\sigma_{ff}(s) = \frac{12\pi s}{m_Z^2} \frac{\Gamma_{ee} \Gamma_{ff}}{(s - m_Z^2)^2 + (m_Z \Gamma_Z)^2} \quad (143)$$

The partial widths are described in the previous section. Here we are ignoring the kinematic effects due to m_f (i.e. assuming the final state fermions are massless)

- Measuring $\sigma_{ff}(s)$ as a function of s at LEP was slightly complicated by the effects of γ ISR/FSR, which can change the kinematics quite a bit. Unlike QCD ISR/FSR, this can be calculated to high precision in QED, and the change in the shape of the Z -peak can be predicted accurately.

- LEP measured:

$$m_Z = 91.1875 \pm 0.0021 \text{ GeV}, \quad \Gamma_Z = 2.4952 \pm 0.0023 \text{ GeV} \quad (144)$$

- The value of Γ_Z can be used to constrain the number of neutrino generations lighter than $m_Z/2$ (assuming universal coupling). It is found to be 3
- The value of Γ_{ff} can be extracted by measuring the cross-section of the decay to $f\bar{f}$ and using the equation:

$$\max_s \sigma_{ff}(s) = \frac{12\pi}{m_Z^2} \frac{\Gamma_{ee}\Gamma_{ff}}{\Gamma_Z^2} \quad (145)$$

- The weak mixing angle can be extracted from c_V, c_A :

$$c_V = I_W^3 - 2Q \sin^2 \theta_W, \quad c_A = I_W^3 \quad (146)$$

The vector and axial components have different angular dependencies, so one can look at the forward-backward asymmetry for a particular type of decay (such as leptons). Define σ_F (σ_B) as the cross-section for $e^-e^+ \rightarrow Z \rightarrow \ell^+\ell^-$, where the ℓ^- is in the forward (backward) region of the detector. Then, one measures:

$$A_{FB} = \frac{\sigma_F - \sigma_B}{\sigma_F + \sigma_B} \quad (147)$$

The measured value is:

$$\sin^2 \theta_W = 0.23146 \pm 0.00012 \quad (148)$$

12.4.3 Measurement of W properties

- The energy at LEP was raised up to $\sqrt{s} > 161$ GeV to facilitate $e^-e^+ \rightarrow W^+W^-$ production
- Branching fractions can be evaluated by looking at full-hadronic decays
 - In doing so, we assume that the W s are on-shell (ignoring the width)
 - The measured branching fraction is:

$$BR(W \rightarrow q\bar{q}') = 67.41 \pm 0.27\% \quad (149)$$

- To measure m_W, Γ_W , we need to assume the W s are virtual:

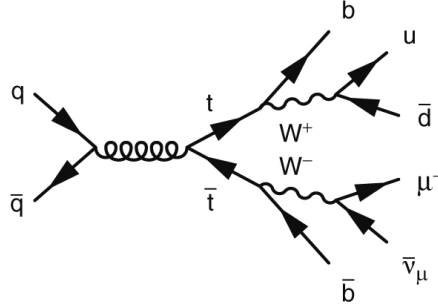
$$|\mathcal{M}|^2 \propto \frac{1}{(q_1^2 - m_W^2)^2 + (m_W\Gamma_W)^2} \times \frac{1}{(q_2^2 - m_W^2)^2 + (m_W\Gamma_W)^2} \quad (150)$$

- LEP looked at fully-hadronic and semi-hadronic decays. The ν -momentum was reconstructed by looking at \vec{E}
- m_W was also measured at the Tevatron, using $p\bar{p} \rightarrow WX$, where X is ISR
 - Was measured in hadronic and leptonic channels
 - In the leptonic case, the fit was done to the m_W^T (transverse mass), not m_W shape
 - Γ_W was also extracted from the width of the m_W^T shape
- The measured properties (LEP+Tevatron) are:

$$m_W = 80.376 \pm 0.033 \text{ GeV}, \quad \Gamma_W = 2.195 \pm 0.083 \text{ GeV} \quad (151)$$

12.4.4 Measurement of t -quark properties

- Discovered in $q\bar{q} \rightarrow t\bar{t}$ channel at Tevatron, where $t \rightarrow bW^+$



- Branching fraction is ~ 1 because $|V_{tb}| \sim 1$
- Lowest-order width is $\Gamma_t = 1.5$ GeV
- Mass was measured in three channels: fully-hadronic, semi-leptonic, and fully-leptonic
- Measured values:

$$m_t = 173.5 \pm 1.0 \text{ GeV}, \quad \Gamma_t = 2.0 \pm 0.6 \text{ GeV} \quad (152)$$

- Using these measured values and m_W , restrictions can be made on the Higgs mass
 - Because loop corrections involving Higgses will affect measured values of m_t, m_W
 - Constraints from LEP and Tevatron are $50 \leq m_H \leq 150$ GeV

13 The Higgs boson

- Cannot add mass terms for gauge bosons or fermions in the Standard Model Lagrangian
- Adding a mass term of the form $m_W^2 W^\mu W_\mu$ is not gauge-invariant
- Similarly, a fermion mass term does not respect $SU(2)_L$:

$$m^2 \bar{\psi} \psi = \frac{m^2}{2} (\bar{\psi}_R \psi_L + \bar{\psi}_L \psi_R) \quad (153)$$

- Therefore, need an alternative way to generate masses

13.1 The Higgs mechanism in the Standard Model

- We add two complex scalars ϕ^+ and ϕ^0 to the SM Lagrangian. They reside in a $SU(2)_L$ doublet:

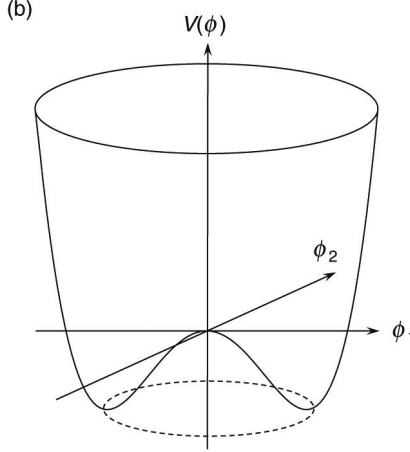
$$\phi = \begin{pmatrix} \phi^+ \\ \phi^0 \end{pmatrix} \equiv \frac{1}{\sqrt{2}} \begin{pmatrix} \phi_1 + i\phi_2 \\ \phi_3 + i\phi_4 \end{pmatrix} \quad (154)$$

where ϕ_i are real.

- The Higgs potential is:

$$V(\phi) = \mu^2 \phi^\dagger \phi + \lambda (\phi^\dagger \phi)^2 \quad (155)$$

As a function of just two components, the potential is:



Note that there are an infinite set of momenta

- The kinetic term for this new field is:

$$\mathcal{L}_{\text{kin}} = (D_\mu \phi)^\dagger (D^\mu \phi), \quad D_\mu = \partial_\mu + ig_W T^a W_\mu^a + ig' \frac{Y}{2} B_\mu \quad (156)$$

- Without loss of generality, we define the vacuum state to be:

$$\langle 0 | \phi | 0 \rangle = \begin{pmatrix} 0 \\ v/\sqrt{2} \end{pmatrix} \quad (157)$$

where $v = -\mu^2/\lambda = 246$ GeV (from experiment).

- We can expand the Higgs field around this vacuum state and choose the unitary gauge to remove the $\phi_{1,2,4}$ degrees of freedom. These dof go into the longitudinal polarizations of W^\pm, Z (which will be necessary once they get mass). The Higgs field is then written as:

$$\phi(x) = \frac{1}{\sqrt{2}} \begin{pmatrix} 0 \\ v + h(x) \end{pmatrix} \quad (158)$$

- If we expand the kinetic term, we see that the W bosons naturally get a mass term (i.e. terms quadratic in W_μ^\pm):

$$m_W = \frac{1}{2} g_W v \quad (159)$$

- If we collect the terms quadratic in W^3, B :

$$\frac{v^2}{8} \begin{pmatrix} W^3 & B \end{pmatrix} \begin{pmatrix} g_W^2 & -g_W g' \\ -g_W g' & g'^2 \end{pmatrix} \begin{pmatrix} W^3 \\ B \end{pmatrix} \quad (160)$$

Diagonalizing the matrix gives the physical A, Z states (eigenvectors) and their masses (eigenvalues):

$$\begin{aligned} A &= \frac{g' W^3 + g_W B}{\sqrt{g_W^2 + g'^2}}, \quad m_A = 0 \\ Z &= \frac{g_W W^3 - g' B}{\sqrt{g_W^2 + g'^2}}, \quad m_Z = \frac{v}{2} \sqrt{g_W^2 + g'^2} \end{aligned} \quad (161)$$

- We can define the weak mixing angle as $\tan \theta_W = g'/g_W$. In terms of this:

$$m_Z = \frac{g_W v}{2 \cos \theta_W} = \frac{m_W}{\cos \theta_W} \quad (162)$$

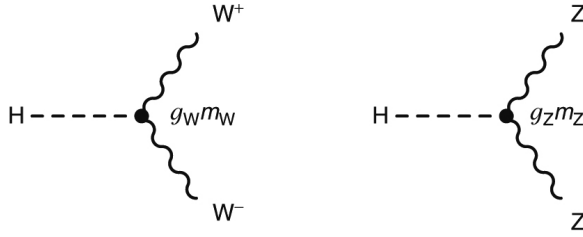
- The Higgs boson mass (corresponding to the h field) is $m_H^2 = 2\lambda v^2$

13.2 Gauge boson masses and interactions

- As mentioned above, m_W, m_Z, m_A are generated through Higgs mechanism:

$$m_W = \frac{g_W v}{2}, \quad m_Z = \frac{g_W v}{2 \cos \theta_W}, \quad m_A = 0 \quad (163)$$

- In the Lagrangian, we can replace v with $h(x)$ in the above mass terms to get $H \rightarrow W^+W^-$ and $H \rightarrow ZZ$ vertices. The strength of the interaction is obviously proportional to m_W and m_Z , respectively. Note there is no $H \rightarrow \gamma\gamma$ vertex because $m_A = 0$



- There are also quartic $HH \rightarrow VV$ interactions for $V = W, Z$

13.3 Fermion masses and interactions

- Let us first consider a left-handed doublet L . Let R be the right-handed singlet corresponding to the $I_W^3 = -1/2$ (i.e. bottom) component of L .
- The term combination $\bar{L}\phi$ is invariant under $SU(2)_L$
- If we write $\phi(x)$ in the unitary gauge after breaking the symmetry (i.e. $\frac{1}{\sqrt{2}}(0, v + h(x))^T$), then $\bar{L}\phi R$ and $\bar{R}\phi L$ are invariant under $SU(2)_L$ and $U(1)_Y$
- This allows us to write mass terms (say for the electron) as:

$$-g_e \left[\begin{pmatrix} \bar{\nu}_e & \bar{e} \end{pmatrix}_L \phi e_R + \text{h.c.} \right] = -\frac{g_e v}{\sqrt{2}} \bar{e} e - \frac{g_e}{\sqrt{2}} h \bar{e} e \quad (164)$$

where g_e is the Yukawa coupling. The value of g_e is chosen so that $m_e = g_e v / \sqrt{2}$. Note that as a consequence of this mass term, we also get a $H \rightarrow ee$ interaction whose strength is m_e/v .

- The above mechanism gives masses (and $H \rightarrow ff$ interactions) for all fermions with $I_W^3 = -1/2$. For $I_W^3 = +1/2$ fermions, we use the same type of interaction, but make the replacement:

$$\phi \rightarrow \phi_C = C\phi = -i\sigma_2\phi^* \quad (165)$$

which selects the top component of the left-handed doublets. Then, we may write:

$$-g_u \left[\begin{pmatrix} \bar{u} & \bar{d} \end{pmatrix}_L \phi_C u_R + \text{h.c.} \right] = -m_u \bar{u} u - \frac{m_u}{v} h \bar{u} u \quad (166)$$

13.4 Decays of the Higgs boson

- Because of the Yukawa coupling $g_b \propto m_b$, the decay $H \rightarrow b\bar{b}$ is dominant:

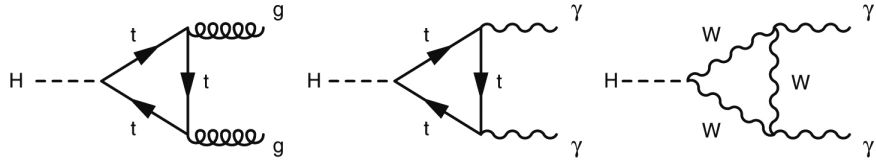
$$\Gamma(H \rightarrow b\bar{b}) = 3 \frac{m_b^2(q^2)m_H}{8\pi v^2} \quad (167)$$

where we have to take into account the running of $\alpha_S(q^2)$. $m_b(m_H^2) \sim 3$ GeV. We can get the other fermion decays by:

$$\Gamma(H \rightarrow f\bar{f}) = \Gamma(H \rightarrow b\bar{b}) \times \frac{N_C^f}{N_C^b} \times \frac{m_f^2(m_H^2)}{m_b^2(m_H^2)} \quad (168)$$

where N_C^f are the number of colors of fermion f .

- The next largest decay is to WW . Although $m_H < 2m_W$ (implying at least one of the W s will be off-shell), the large $g_W m_W$ coupling makes this BR large
- There can also be effective couplings for $H \rightarrow gg, \gamma\gamma$, despite these bosons being massless:



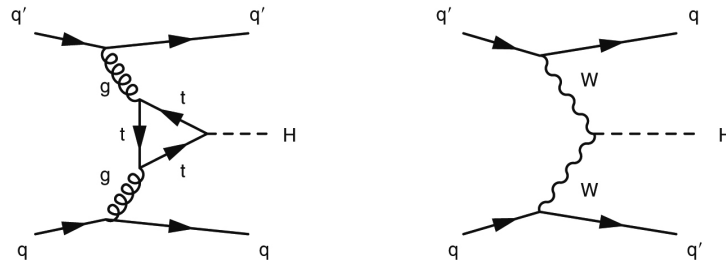
Despite being loop-suppressed, these decays are significant because g_t and $g_W m_W$ are large.

- The leading decay modes are:

Decay mode	$b\bar{b}$	W^+W^-	$\tau^+\tau^-$	gg	$c\bar{c}$	ZZ	$\gamma\gamma$
BR	57.8%	21.6%	6.4%	8.6%	2.9%	2.7%	0.2 %

13.5 Experimental discovery

- LHC used $p\bar{p}$ collisions at $\sqrt{s} = 7, 8$ TeV
- Dominant production mechanism is gluon fusion, but vector boson fusion is easy to identify due to two jets at high $|\eta|$:



- Gluon fusion is sensitive to the gluon PDFs
- Sensitive channels during discovery where $\gamma\gamma, ZZ \rightarrow 4\ell, WW \rightarrow 2\ell 2\nu, \tau\tau$ (hadronic and leptonic), and $b\bar{b}$
- The measured mass is:

$$m_H = 125.7 \pm 0.5 \text{ GeV} \quad (169)$$

14 Dark matter

14.1 Astrophysical evidence for DM

- We proceed in order of decreasing scale
- Temperature anisotropies in CMB

- Measured by WMAP, Planck
- CMB arises from 4×10^5 years after Big Bang
- Power spectrum of fluctuations is sensitive to amount of dark matter and dark energy at this time
- Λ CDM is the cosmological model that fits the data the best, predicting a non-zero cosmological constant Λ and dark matter with a small random velocity (i.e. cold)
- From size of anisotropies, can estimate energy densities:

$$\Omega_b \sim 0.05, \quad \Omega_{\text{DM}} \sim 0.25, \quad \Omega_{\Lambda} \sim 0.7 \quad (170)$$

- Gravitational lensing
 - For example: if a galaxy is between the Earth and an object being studied, the galaxy can bend spacetime so the shortest path between the Earth and the object is around the object
 - Can lead to deformations of the image (weak lensing) or multiple copies of the image (strong lensing)
 - Mass predicted from strength of lensing is $\sim 200\times$ the luminous mass
- Bullet cluster
 - Small cluster passing through larger cluster 3.7 billion light-years away
 - Can use weak lensing to map distribution of matter \Rightarrow consistent with a dark matter halo
 - In particular, the lensing does not follow the distribution of baryonic matter, indicating MOND is not correct
- Rotational velocities of stars in galaxies
 - Objects outside bulk of visible mass distribution should have velocities $v \propto r^{-1/2}$
 - Rubin found this was not the case: v does not drop off after the end of the visible matter bulk
 - Can be solved by adding a dark matter halo around the galaxy
 - Similar results seen in velocities of clusters in nebulae by Zwicky
 - * First hint of DM

14.2 Candidates

- MOND and relativistic extensions largely seen as insufficient to explain all observations or generate a stable Universe
- MACHOs are things like neutron stars, brown dwarfs, black holes, ...
 - Searches using gravitational microlensing puts an upper limit on MACHOs comprising no more than 20% of DM density
 - Measurements of light element abundances (e.g. deuterium, which is only produced during Big Bang nucleosynthesis), constrains $\Omega_b \sim 0.04$
- Neutrino-related candidates
 - Neutrinos are a candidate, but due to mass and relativistic velocity in early Universe, not consistent with clustering scale of galaxies
 - Sterile neutrinos are another candidate
 - * Right-handed, so does not affect Z-width. Can be used to generate neutrino masses through seesaw mechanism

- * Can be cold (non-relativistic) or warm (relativistic in early Universe)
- Weakly interacting massive particles are a good candidate
 - If we assume the DM particle interacts with the weak force (or has a weak-scale interaction), then the relic density mean the mass must be ~ 0.1 GeV - 1 TeV
 - Typically assume WIMPs and baryons were in equilibrium in early Universe
 - Universe temperature then fell below WIMP mass \Rightarrow baryons \rightarrow WIMP stops
 - Expansion stops WIMP \rightarrow baryons when the annihilation rate is less than the Hubble expansion rate
 - The WIMP density at this point is the relic density
 - Alternatively can phrase WIMP miracle as: if we assume the mass is ~ 0.1 GeV - 1 TeV, to reproduce the currently-observed dark matter density, the interaction must be weak-scale
 - Candidates:
 - * Neutralino from SUSY with R -parity (or other LSP)
 - * Lightest Kaluza-Klein mode from compactified extra dimensions, if we impose a KK parity
- Finally, axions
 - Scalar massive particle used to solve strong CP problem
 - * Quantize the Θ parameter in the QCD Lagrangian that controls CP violation
 - * Break the symmetry of this field \Rightarrow pseudo-Nambu-Goldstone boson (axion)
 - Also a cold DM candidate

14.3 Overview of searches

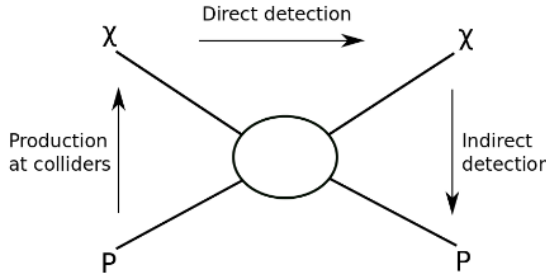


Figure 1. Schematic showing the possible dark matter detection channels.

14.4 Direct detection

- Signature is nuclear recoil from $\chi N \rightarrow \chi N$
- If we assume $10 < m_\chi < 10^3$ GeV, then the recoil is $1 < R < 100$ keV.
- The recoil spectrum is:

$$\frac{dR}{dE}(E) = \frac{\rho_0}{m_\chi M_A} \int d^3v \left[v f(\vec{v}) \cdot \frac{d\sigma}{dE}(E) \right] \quad (171)$$

where

- E is the DM energy
- ρ_0 is the local DM density and $f(\vec{v})$ is the local DM velocity distribution
- M_A is the target nucleus mass

- We can add an annual modulation to account for the Earth's motion:

$$\frac{dR}{dE}(E, t) \sim S_0(E) + S_m(E) \cdot \cos\left(\frac{2\pi}{T}(t - t_0)\right) \quad (172)$$

14.4.1 Cross-sections

- If the interaction is spin-independent (i.e. scalar or vector mediator), then isospin conservation \Rightarrow neutrons and protons contribute equally to $\sigma_{\chi N}$
- For spin-dependent interactions, need unpaired nucleons \Rightarrow use odd-even or odd-odd nuclei
- Let σ_0 and F be the cross-section (at zero momentum transfer) and form factor, respectively. Then, the total cross-section is:

$$\frac{d\sigma}{dE} = \frac{M_A}{2\mu_A^2 v^2} \cdot (\sigma_0^{\text{SI}} F_{\text{SI}}^2(E) + \sigma_0^{\text{SD}} F_{\text{SD}}^2(E)) \quad (173)$$

where μ_A is the reduced mass of the χ -nucleus system.

- We can write the spin-independent cross-section as:

$$\sigma_0^{\text{SI}} = \sigma_p \cdot \frac{\mu_A^2}{\mu_p^2} \cdot [Z f^p + (A - Z) f^n]^2 \quad (174)$$

where:

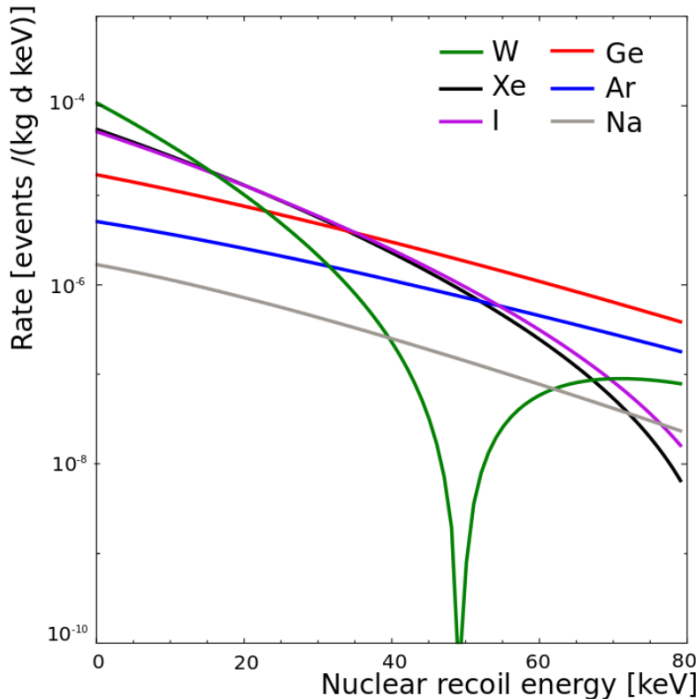
- * f^p (f^n) is the interaction strength with protons (neutrons)
- * μ_p is the reduced mass of the χ -nucleon system
- * Typically assume $f^p = f^n = 1$, so σ_p controls the cross-section

- The spin-dependent cross-section is:

$$\sigma_0^{\text{SD}} \propto \mu_A^2 [a_p \langle \mathbf{S}^p \rangle + a_n \langle \mathbf{S}^n \rangle]^2 \frac{J+1}{J} \quad (175)$$

where J is the nucleus spin

- If we assume a spin-independent interaction with $m_\chi = 100$ GeV and $\sigma = 10^{-45}$ cm 2 :



- The local DM density is typically:

$$\rho_0 = 0.2 - 0.6 \frac{\text{GeV}}{\text{cm}^3} \quad (176)$$

- If we assume an isotropic Maxwell-Boltzmann distribution:

$$f(\mathbf{v}) = \frac{1}{\sqrt{2\pi}\sigma} \exp\left[-\frac{v^2}{2\sigma^2}\right], \quad \sigma = \sqrt{\frac{3}{2}}v_c \quad (177)$$

where f is the velocity distribution in the rest frame of the galaxy, and $v_c = 220 \text{ km/s}$ is the circular velocity of an object at this distance from the center of the galaxy. We find $v_{\text{RMS}} = 270 \text{ km/s}$.

- The flux is therefore:

$$\Phi_\chi = \frac{\rho_0}{m_\chi} \langle v \rangle \sim \frac{0.4 \text{ GeV/cm}^3}{100 \text{ GeV}} \times 270 \frac{\text{km}}{\text{s}} \sim 10^5 \text{ cm}^{-2}\text{s}^{-1} \quad (178)$$

14.4.2 Backgrounds

- γ decays

- Common isotopes in environment can give γ s with $E_\gamma \sim 10 \text{ keV} - 2.6 \text{ MeV}$
- Can be limited by using active materials whose radioactive isotopes are rare (Ge or Xe, for example)
- Can add shielding to prevent γ s from environment.
 - * Something with high Z and ρ (i.e. Pb) to increase pair-production and photoelectric σ s in the shielding.
 - * Can also use large water tank
- Depending on the detector, offline discrimination can be done
 - * γ s more likely to interact multiple times in detector (i.e. through Compton or secondary interactions from e s from photoelectric or pair-production)
 - * If a scintillator, can use pulse-shape discrimination

- Neutrons

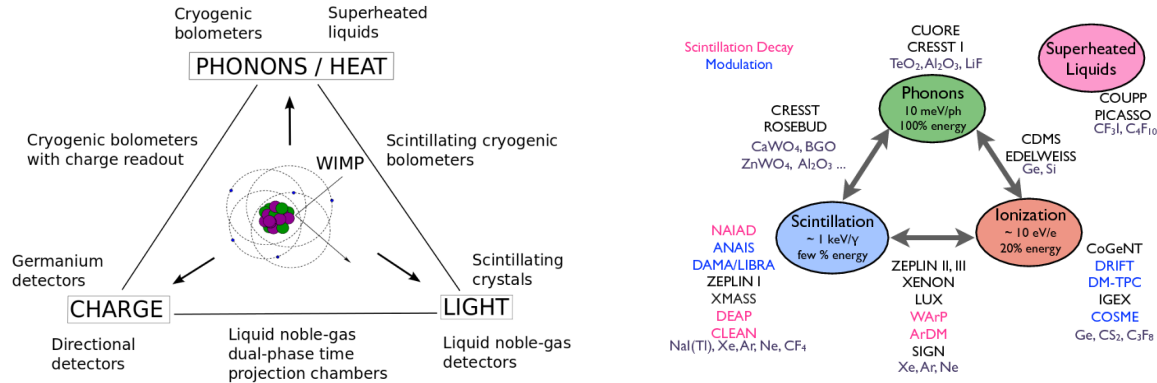
- From radioactive decay or cosmic ray μ s spallation on surrounding material
- Energies are from $\sim \text{MeV}$ (radiogenic) to $\sim \text{GeV}$ (cosmogenic)
- High energy neutrons can be moderated in surrounding material to produce recoils of $\sim \text{keV} \Rightarrow$ same signal as DM
- Cosmogenic neutrons can be limited by putting the detector deep underground (reduce flux to $10^{-6} - 10^{-10} \text{ cm}^{-2}\text{s}^{-1}$)
- Radiogenic neutrons can be limited by choosing materials with low radioactivity (including α s, which can lead to (α, n)).
- Can reduce neutron flux:
 - * Add shielding around detector
 - * Active vetos: scintillator or water Cerenkov

- Neutrinos

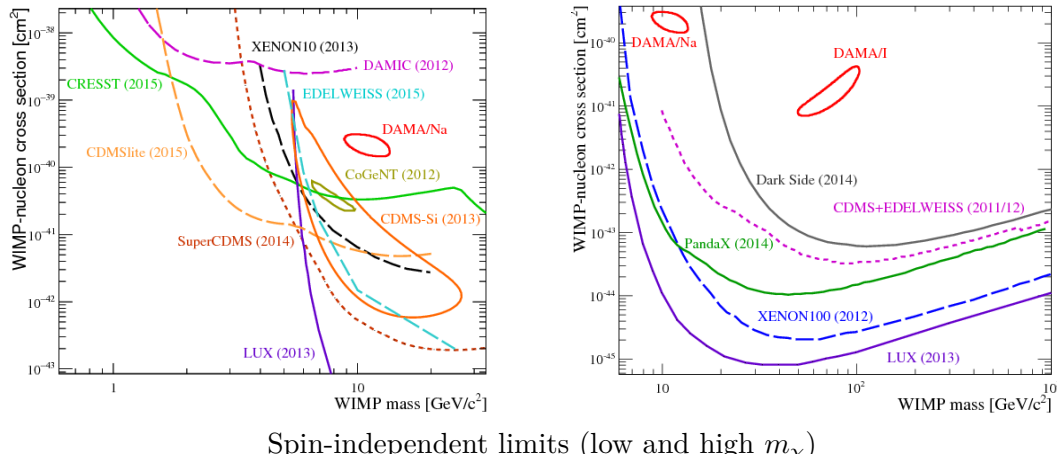
- Can produce signals through electron or nucleon interactions
- Largest fluxes are solar neutrinos: pp and ${}^7\text{Be}$ are biggest sources
- CC and NC interactions with electrons and CC interactions with nucleons can be discriminated against

- * Electron interactions where the recoil is \sim keV are ionizations
- * CC nucleon interactions will have different energy spectra
- Coherent neutrino scattering off nucleons is *irreducible background*
- * Has never been measured

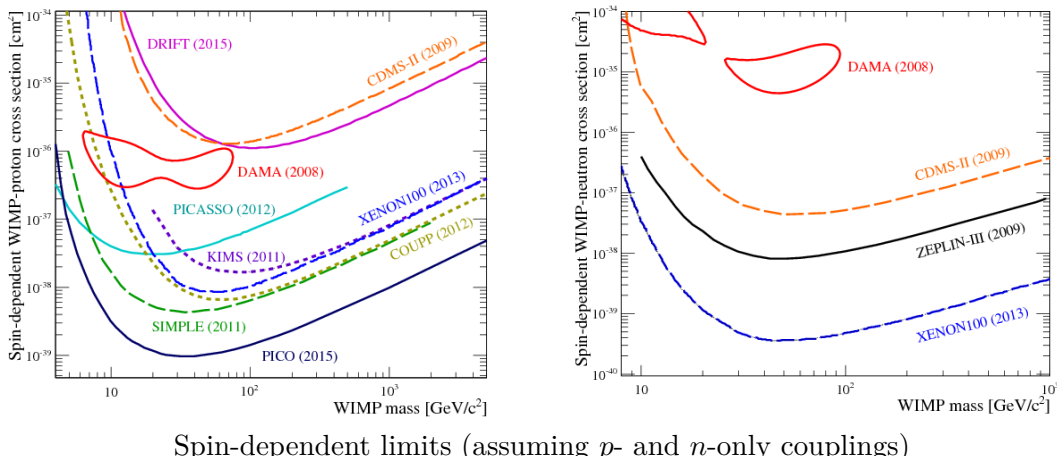
14.4.3 Detector types



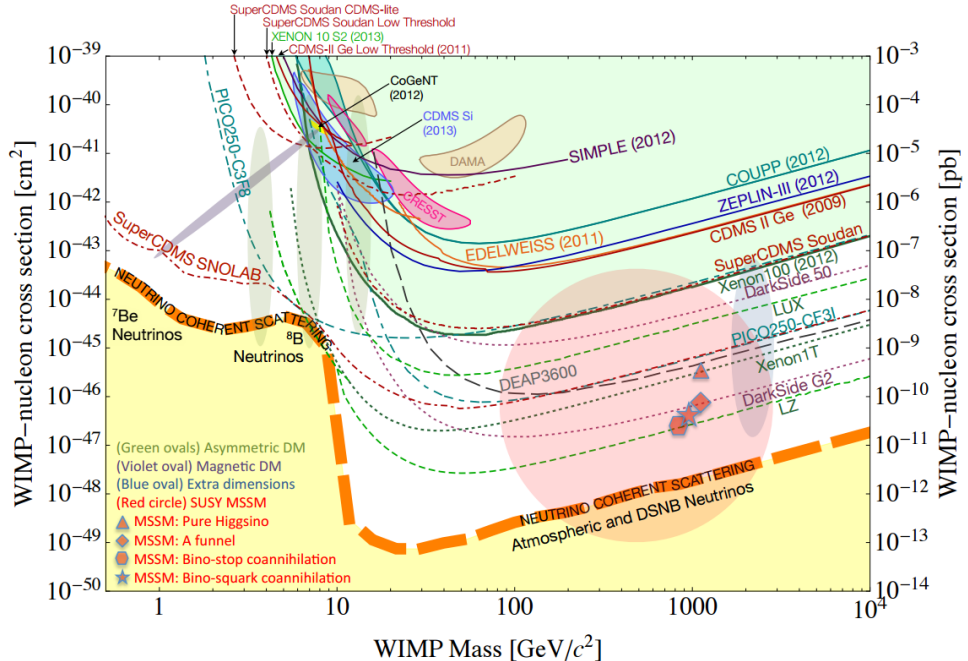
14.4.4 Direct detection limits



Spin-independent limits (low and high m_χ)

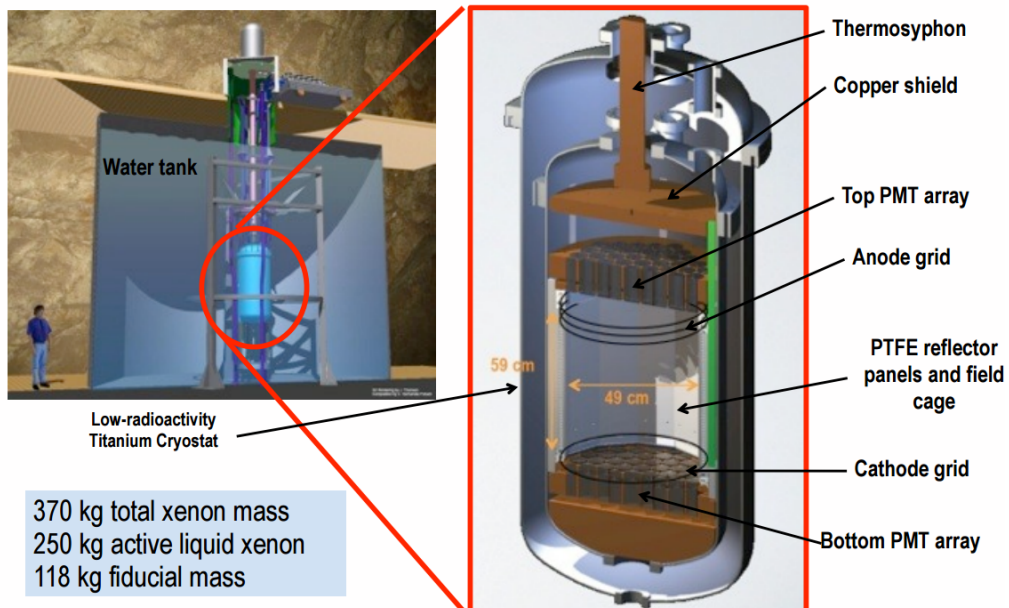


Spin-dependent limits (assuming p - and n -only couplings)



This plot is old, but shows the spin-independent limits in comparison to the neutrino floor

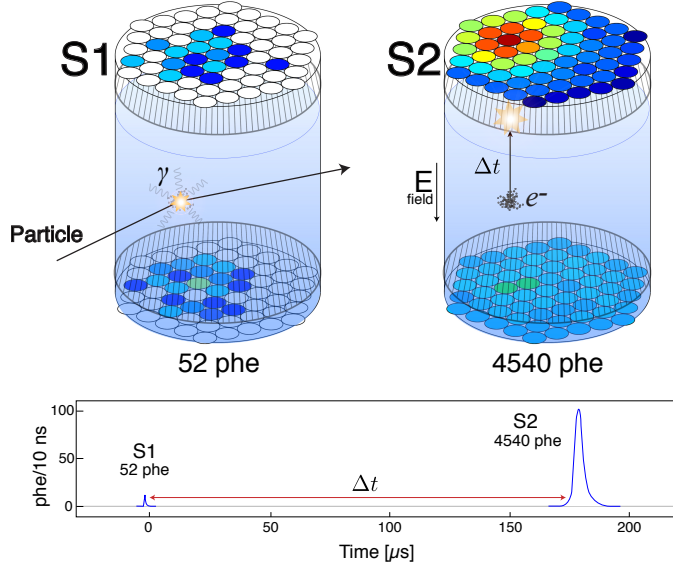
15 Large Underground Xenon experiment



- 370 kg two-phase xenon TPC (~ 118 kg fiducial volume)
- Located 1 mile underground in Homestake
- Placed inside large water tank to block γ and n backgrounds
- $\chi + \text{Xe} \rightarrow \chi + \text{Xe}^*$ interactions generate 175 nm photons and electrons from ionization
 - Prompt photons are picked up by PMTs

- Electrons drift in \vec{E} -field up to Xe gas, where they are accelerated
- Accelerated electrons brem, photons are picked up by PMTs
- Expected sensitivity was spin-independent cross section of $2 \times 10^{-46} \text{ cm}^2$ or ~ 0.5 events/100 kg/month

15.1 Signal signature



- $\chi + \text{Xe} \rightarrow \chi + \text{Xe}$ event generates photons and electrons
- Photons are from scintillation: Xe atom is excited and then de-excites.
- Characteristic 175 nm photons are pick up by PMTs. This signal is mostly used for figuring out t_0 , as the radiation is isotropic and does not specify position. Order of 50 photoelectrons
- Electrons drift upwards towards gaseous region
- Electrons are accelerated due to stronger \vec{E} -field in gaseous part of the TPC. They release photons due to acceleration, which are roughly aligned with direction of motion
- These photons are picked up by top PMTs. Time light reaches PMTs is t_1 . Localization of light specifies position in x - y plane. Typically release $\sim 4.5 \times 10^3$ photoelectrons
- Use $(t_1 - t_0)/v$ to determine position of interaction along z axis.
- Look for events whose deposited energy (from the scintillation + electrons released) is in the range 3.4-25 keV_{NR} (where the NR subscript refers to the energy reconstructed assuming a nuclear recoil)
- Position accuracy is ~ 1 cm (x - y) and \sim mm (z)

15.2 Detector components

15.2.1 Water tank and muon tagging

- 7×6 m water tank to shield from:

- γ s
- Neutrons from cavern radioactivity

- High-energy neutrons from μ interactions
- Instrumented with 20 large PMTs to identify γ s from muons (Cerenkov radiation or hadronic showers)
 - Any TPC event that is simultaneous to a water tank event is rejected

15.2.2 Cryogen

- Cools the entire detector (active volume, anode/cathode, PMTs)
- Two phase system: gaseous and liquid N₂
- 4 total cool heads:
 - 2 bring the detector down to 175 K
 - 2 maintain a thermal gradient along vertical axis (to facilitate two states of Xe)

15.2.3 Xenon

- Active area (liquid Xe) has a height of 49 cm and diameter of 50 cm. Above this is a 10 cm tall volume of Xe gas.
- Density of liquid is 2.9 g/cm³
- Liquid Xe is continuously purified to maintain electron drift length
- Use a purifier that requires gaseous Xe \Rightarrow use a dual-phase heat exchanger to evaporate and condense Xe

15.2.4 TPC \vec{E} -field

- TPC is surrounded by polyethylene reflector panels that allow total internal reflection of scintillation
- A copper disk is mounted on top of TPC. It is connected to the cryogen and serves as a heat sink for the cables, as well as a shield against γ s
 - An additional copper structure is on the bottom of the TPC
- 61 PMTs are mounted above and below TPC
 - Areas between PMT faces are covered with polyethylene reflectors
- 5 wire grids, in order from bottom to top:
 1. 2 cm above bottom PMTs is a grid to shield the PMTs from the cathode grid. The voltage is tuned so that the \vec{E} -field at the PMT photocathode surface is zero
 2. 4 cm above bottom PMTs is the cathode grid. It generates a 2 kV/cm drift field in the liquid
 3. 5 mm below the liquid surface is the gate grid used to generate a 5 kV/cm \vec{E} -field (below liquid surface, used to extract electrons) and 10 kV/cm \vec{E} -field (in gas volume, used to accelerate electrons)
 4. 1 cm above gate grid is the anode grid.
 5. 4 cm above anode and 2 cm below top PMTs is another shielding grid.
- Along the length of the TPC are copper rings (1 cm apart) that are held at voltages to maintain the drift field at a constant value

15.2.5 PMTs and light collection

- Two arrays of 61 PMTs.
 - 12 stages
 - Gain: $\sim 10^6$
 - Rise time: ~ 3 ns
 - QE at 175 nm: 33%. collection efficiency: 90%
 - Operating voltage: 1.1 kV
 - Peak QE is at 175 nm
- Using likelihood pattern recognition techniques, position accuracy in x - y plane of S2 signal is ~ 1 cm (20% of PMT diameter)
- Significant source of background is PMT radioactivity
 - Measured using a high-purity Ge detector. Biggest sources are ^{40}K (65 mBq) and ^{238}U (10 mBq)
- Light collection efficiency
 - High UV-reflective polyethylene panels surround TPC to minimize light leakage
 - The 5 grids are 88-99% transparent and are slightly reflective
 - Used 662 keV photons from ^{137}Cs to determine efficiency of 8 photoelectrons/keV_{ee}
 - * keV_{ee} is the reconstructed energy assuming an electron event (i.e. electron-equivalent)

15.2.6 Triggering

- Three modes: S1, S2, or S1&S2
- Trigger dead time is up to 8 μs

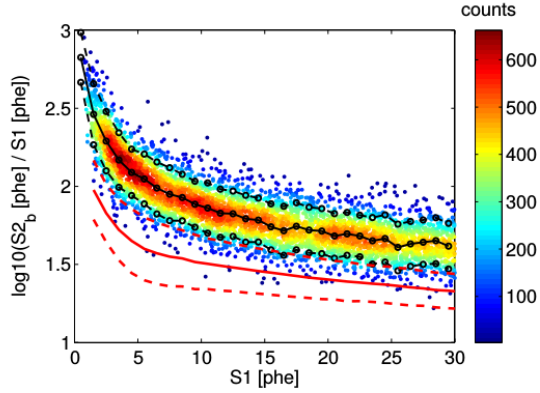
15.3 Background sources and rejection

- As described above, cosmogenic backgrounds (i.e. cosmic ray μs) are shielded and identified using the instrumented water tank.
- Here we discuss radiogenic backgrounds

15.3.1 Electron recoils

- Dominant background
- From photons or electrons (mostly photons)
 - γs or βs come from radioisotope decays in detector or Xe itself (although later is very rare)
 - Anything outside the water tank is heavily shielded against
 - Liquid Xe attenuates photons with $\lambda = \mathcal{O}(1)$ cm, so can reject events near edge of TPC
 - * Energies are $\mathcal{O}(0.1)$ - $\mathcal{O}(1)$ MeV
- LUX signal range (discussed above) corresponds to 0.9-5.3 keV_{ee}
- ER events release many more electrons (increasing S2) than scintillation photons (which are from nuclear recoil)

- Therefore, a 2D cut is applied on $\ln(S2/S1)$ and S1
- In the following plot, the data points are ER events (tritium β decay) and the solid red curve is the mean of (simulated) NR events:

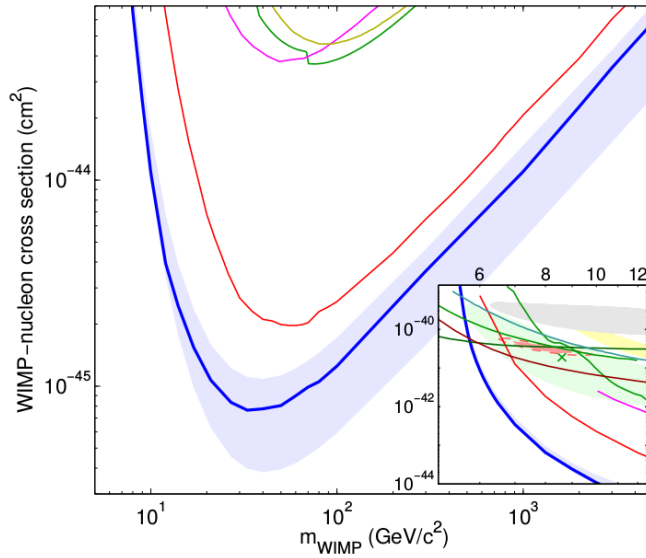


15.3.2 Non-DM nuclear recoils

- From neutron scattering events
- Neutrons typically come from (α, n) interactions in detector or ^{238}U fission
 - Energies are $\sim \text{MeV}$
- Can also come from cosmic muons
 - These are $\sim \text{GeV}$ and have mean free path much longer than size of the detector
- Difficult to discriminate against, as the signature is essentially identical to DM
- If the energy is low enough, σ_{nN} is large enough that multiple scatterings expected
 - So reject events with multiple displaced signals

15.4 2013 results

- Did a unblinded run of 85.3 live-days
- Set limits on spin-independent $\sigma_{\chi N}$ as a function of m_χ
- Best current limits for $6 < m_\chi < 10^3 \text{ GeV}$



LUX (blue curve) limits compared to XENON100 (red and orange) and other experiments

16 Non-DM BSM

- Graviton
 - Particle excitation of gravitational field
 - Corresponds to quantization of $T_{\mu\nu} \Rightarrow$ spin 2
 - Have not seen yet since the coupling is very small
 - Can look for \cancel{E}_T at colliders, resonant production of G, \dots
- Supersymmetry
 - Z_2 symmetry between particles and superpartners

SM spin	MSSM spin
1/2	0
1	1/2
0	1/2
2	3/2

 - If the symmetry were unbroken, particles and superpartners would have the same mass
 - Hierarchy problem: $G_F/G_N \sim 10^{32}$
 - * Equivalent to saying $m_H \ll m_{\text{Planck}} \equiv G^{-1/2} \sim 10^{19} \text{ GeV}$
 - * To get such a small (observed) value of m_H , the bare mass must be huge
 - * Loop corrections from top quark are $\sim 10^{16} \text{ GeV}$, but $m_H \sim 10^2 \text{ GeV} \Rightarrow$ quantum corrections are on the order of the bare mass
 - * If there are sfermions, then the loop corrections from fermions and sfermions can destructively interfere
- Large ED
 - $4 + \delta$ dimensions

- * SM fields propagate in 4D gravity in $(4 + \delta)D$
- Then we get Kaluza-Klein modes for the graviton
- Experimental searches:
 - * Changing power law at small scales, i.e. violation of $F \propto 1/r^2$
 - * Graviton is produced and propagates in ED before decaying $\Rightarrow \not{E}_T$

17 Nuclear physics

17.1 β^- decay

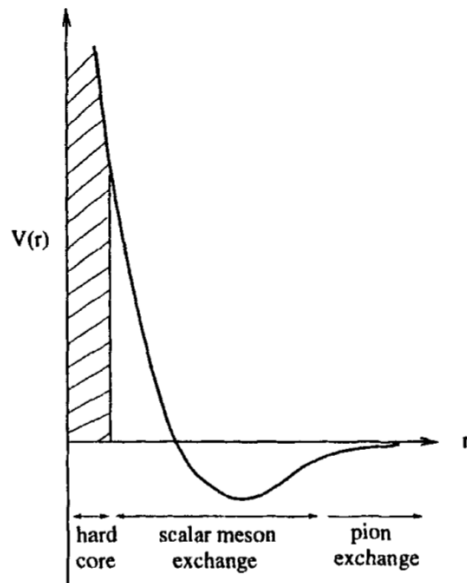
- Allowed decays have non-zero matrix elements at LO
 - Fermi decays are the vector part of the current
 - * $\Delta J = \Delta I = \Delta P = 0$
 - * $\Delta I_3 = \pm 1$
 - Gamow-Teller decays are axial-vector
 - * $\Delta J = 0, \pm 1$ (but not $0 \rightarrow 0$)
 - * $\Delta I = 0, \pm 1$ (but not $0 \rightarrow 0$)
 - * $\Delta I_3 = \pm 1$
 - Superallowed decays are $0^+ \rightarrow 0^+$
- Forbidden decays have non-zero matrix elements at only $N(N\dots)LO$
 - Can have wilder variations in $\Delta J, I$

17.2 Nuclear isospin

- Pions are the isospin triplet
- (p, n) are an isospin doublet
- Therefore, an np system has $T = 0, 1$, but a pp system has $T = 1$
- $d(np)$ is the antisymmetric $T = 0$ singlet

17.3 NN interactions

Figure 3-7: Schematic diagram showing the different parts of a nucleon-nucleon potential as a function of distance r between two nucleons. The hard core radius is around 0.4 fm and it takes energy >1 GeV to bring two nucleons closer than (twice) this distance. The main part of the attraction lies at intermediate ranges, at radius ~ 1 fm, and is believed to be dominated by the exchange of scalar mesons. The long-range part, starting at around 2 fm, is due to the single-pion exchange.

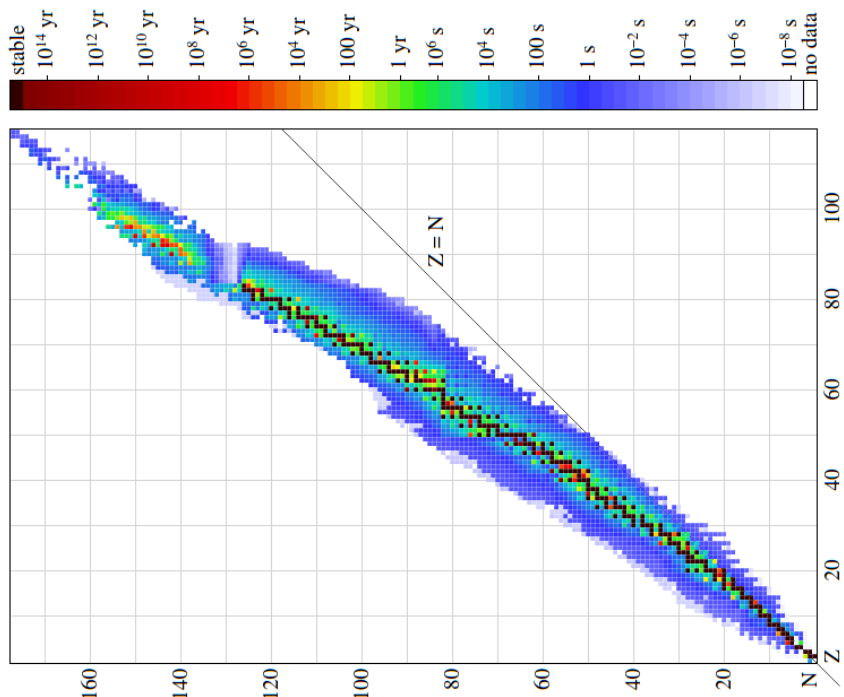


- Three regimes: hard-core, scalar meson-exchange, 1 π -exchange
- The scalar-meson exchange is due to exchange of multiple π s or heavier mesons
- Single-pion exchange is modeled by Yukawa interaction:

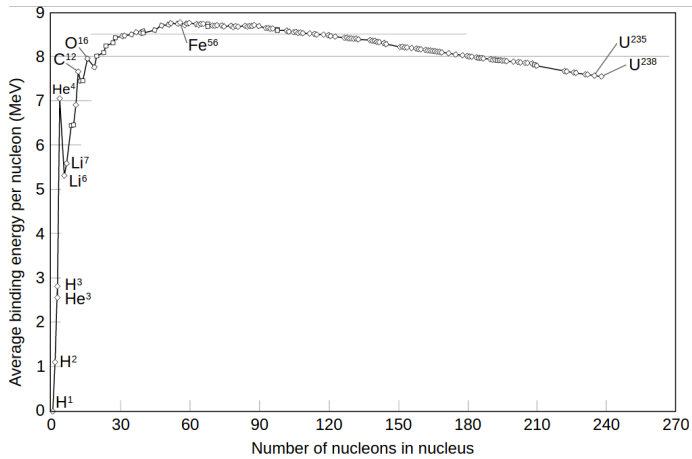
$$V(r) = \frac{g}{4\pi} \frac{1}{r} e^{-m_\pi r} \quad (179)$$

- This is the potential due to leading-order interactions arising from a πNN term in the Lagrangian

17.4 Nuclear models



17.4.1 Liquid drop model



- Assume constituents of nucleus are much smaller than nucleus \Rightarrow drop of incompressible fluid
- \Rightarrow Semi-empirical mass formula: $E_B(Z, N) = \alpha_1 A - \alpha_2 A^{2/3}$
 - where A is the volume term
 - and $A^{2/3}$ is the surface tension term
- The full mass-formula is:

$$E_B(Z, N) = \alpha_1 A_1 - \alpha_2 A^{2/3} - \alpha_3 A^{-1/3} - \alpha_4 \frac{(N - Z)^2}{A} + \alpha_5 \Delta \quad (180)$$

- The first two terms are due to the liquid drop model
- The α_3 term is from Coulomb repulsion
- The α_4 term is the symmetry term (prefer $N \sim Z$ at low A)
- The α_5 term is the pairing effect:

$$\Delta = \begin{cases} \delta & \text{even-even} \\ 0 & \text{even-odd or odd-even} \\ -\delta & \text{odd-odd} \end{cases} \quad (181)$$

17.4.2 Shell model

- Like H atom, but potential is (deformed) 3D HO:

$$V(\mathbf{r}) = \frac{\mu\omega^2 r^2}{2} \quad (182)$$

- Energy levels are $\hbar\omega(N + 3/2)$, where the degeneracy in N is $(N + 1)(N + 2)$
 - Shells are $2(N = 0), 6(N = 1), 12(N = 3), \dots$
 - Magic numbers are therefore $2, 8, 20, \dots$
- 3D HO is deformed by spin-orbit interactions
 - Affects magic numbers > 20
 - Shells are split by value of j
 - * Splitting can actually cause N to overlap, e.g. $E_{j=1/2}^{N=3} \approx E_{j=9/2}^{N=4}$
 - * New magics are $2, 8, 20, 28, 50, 82$

17.4.3 Fermi gas model

- Assume nucleons are in a square well of volume V
 - Different potentials for n, p
 - Proton potential is modified a bit for Coulomb interaction

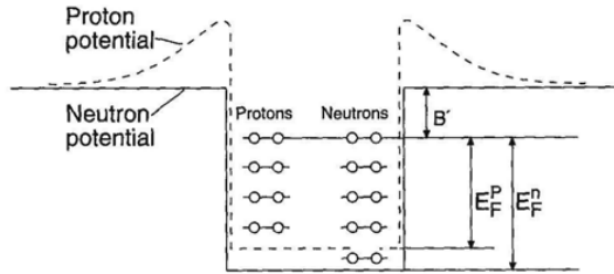


Fig. 8.1. Sketch of the proton and neutron potential wells and states in the Fermi gas model [B. Povh et al., *Particles and Nuclei*, Springer, 2002].

- The number of states is:

$$N, Z = \int \int \frac{d^3r}{(2\pi\hbar)^3} \frac{d^3p}{(2\pi\hbar)^3} = \frac{V}{(2\pi\hbar)^3} \frac{4\pi}{3} (k_F^{n,p})^3 \quad (183)$$

where k_F is the Fermi momentum

- We find the Fermi energy is:

$$E_F^{p,n} = \frac{(p_F^{p,n})^2}{2m_{p,n}} \approx 33 \text{ MeV} \quad (184)$$

- Since $E_B/A \sim 7\text{-}8 \text{ MeV}$, the depth of the square potential is $\sim 40 \text{ MeV}$

17.5 Solar processes

- Mean time for a photon to get from the center of the sun to the edge of the outer core is 10^5 years. This is due to multiple scattering off e^-

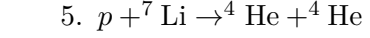
17.5.1 PP processes

- Most of the energy of the sun
- $4p \rightarrow {}^4\text{He}$
- First steps (total of 7 MeV released):

1. $2 \times (p + p \rightarrow d + e^+ + \nu_e)$, occurs at $T \sim 2 \text{ keV}$ so d is stable
2. $2 \times (p + d \rightarrow {}^3\text{He} + \gamma)$

- PPI (13 MeV released)
 3. ${}^3\text{He} + {}^3\text{He} \rightarrow {}^4\text{He} + p + p$

- PPII (20 MeV released)
 3. ${}^3\text{He} + {}^4\text{He} \rightarrow {}^7\text{Be} + \gamma$
 4. ${}^7\text{Be} + e^- \rightarrow {}^7\text{Li} + \nu_e$



- PPIII (18 MeV released)
 3. ${}^3\text{He} + {}^4\text{He} \rightarrow {}^7\text{Be} + \gamma$
 4. $p + {}^7\text{Be} \rightarrow {}^8\text{B} + \gamma$
 5. ${}^8\text{B} \rightarrow {}^8\text{Be} + e^+ + \nu_e$
 6. ${}^8\text{Be} \rightarrow {}^4\text{He} + {}^4\text{He}$

17.5.2 CNO cycle

- Uses a C nucleus to turn $4p$ into ${}^4\text{He}$
- Total of 6 steps to go $\text{C} \rightarrow \text{N} \rightarrow \text{O} \rightarrow \text{C} + \alpha$

17.6 Nucleosynthesis

17.6.1 BBN

- 10 s - 20 m after Big Bang
- Mostly ${}^4\text{He}$, plus some ${}^3\text{He}$, D, ${}^7\text{Li}$
- $T \sim 1 \text{ MeV}$
- Freeze out of n, p (i.e. T too low for equilibrium through weak interaction)
 - We find $N_n/N_p \sim 1/7 \sim e^{-Q/T}$ after freeze-out, where $Q = m_n - m_p$
- Abundance of light elements is in good agreement between theory and data

$$\frac{{}^4\text{He}}{\text{H}} \approx 0.08, \frac{{}^7\text{Li}}{\text{H}} \approx 10^{-10} \quad (185)$$

- Can measure these concentrations by looking in regions where there are few stars (which can change element abundance)
- Can measure abundance of D by looking for shifted Lyman- α lines
- Similarly look for emission lines from other elements
- ${}^7\text{Le}$ measurement is in tension with BBN prediction and other light elements
- ${}^4\text{He}$ was produced earlier and in greater abundance than D because D has low binding energy (2.2 MeV). Therefore, γs at thermal eq. could dissociate D easily. Need to wait for Universe to cool to $T \sim 0.1 \text{ MeV}$

17.6.2 Stellar

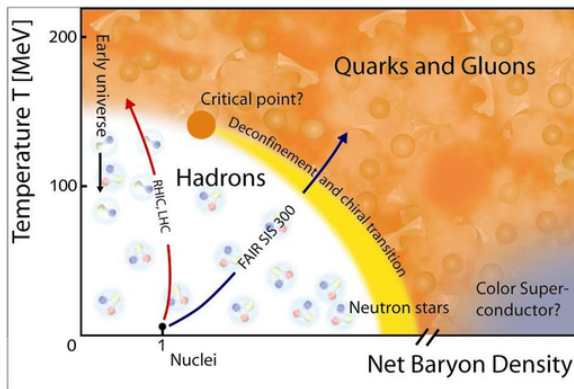
- Heavier elements are produced closer to core ($kT \sim 1 \text{ MeV}$)
- Can only reach ${}^{56}\text{Fe}$ in stars
- The 3α process makes carbon production very easy:
 - $\alpha + \alpha + \alpha \rightarrow {}^{12}\text{C} + \gamma$
 - The ${}^{12}\text{C}$ is in a 0^+ excited state, so the Q value is $\sim 300 \text{ MeV}$

17.6.3 Supernovae

- *s*-process: slow neutron capture in massive stars
- *r*-process: rapid neutron capture in supernovae core collapse
 - High density \Rightarrow free e^- states are filled up to high Fermi energy $\Rightarrow \beta^-$ decay is suppressed
 - High neutron flux (from e^- capture by proton) \Rightarrow nuclei get n -enriched
 - After density decreases, β^- decay proceeds as normal, so Z decreases towards the valley of stability

17.7 Quark-gluon plasma

- Occurs at very high energy and density (or chemical potential)



- Can be studied at heavy-ions collisions (first at SPS, then RHIC and LHC)
- Centrality is a function of the impact parameter of the collision. 0% refers to $b = 0$ and 100% refers to the ions missing each other.

17.7.1 RHIC

- Polarized protons and ions (Cu, Au, U) with $\sqrt{s_{NN}} \leq 200$ GeV
- Evidence for QGP:
 - Perfect fluid with near-zero shear velocity \Leftrightarrow elliptic flow
 - Jet quenching: high p_T partons scatter in QGP before escaping \Rightarrow lower p_T
 - * Find that:

$$R_{AA}^{\text{jet}} \propto \frac{N(\text{jets in } AA \text{ collision}, p_T)}{A^2 N(\text{jets in } pp \text{ collision}, p_T)} < 1 \quad (186)$$

R decreases as a function of A . $R_{AA}^{\text{jet}} \sim 0.5$ and increases a bit at high p_T

* A similar measurement can be done for $R_{AA}^{\gamma, Z \rightarrow \mu\mu}$. These are found to be $\sim 1 \Rightarrow$ QCD interactions cause $R_{AA}^{\text{jet}} < 1$

- Also find cross-section for producing J/ψ is decreased, since the $c\bar{c}$ pairs do not remain confined in the QGP and hadronize with other lighter quarks

17.8 Nuclear reactors

- For example:
 - $^{235}\text{U} \rightarrow ^{92}\text{K} + ^{142}\text{B} + 2n$. Neutrons have energy $\sim \text{MeV}$
 - $n + ^{235}\text{U} \rightarrow ^{92}\text{K} + ^{142}\text{B} + 2n$, etc
- To make the second step work, need $E_n \sim \text{meV}$ to increase neutron capture cross-section. Use moderators like water, heavy water, carbon

Appendices

A Bibliography

Bettini A., *Introduction to elementary particle physics*

The BaBar Collaboration, *The BABAR Physics Book.*

<https://www.slac.stanford.edu/pubs/slacreports/reports19/slac-r-504.pdf>

The CPLEAR Collaboration, *The CPLEAR-Experiment at CERN*. Nucl. Phys. B. 59 (1997) 76-100

The CPLEAR Collaboration, *The CPLEAR detector at CERN*. Nucl. Inst. and Meth. 379 (1997) 182-191

The CPLEAR Collaboration, *The CPLEAR Experiment,*

<https://cplear.web.cern.ch/cplear/cplear/newtransparencies/>

The LUX Collaboration, *The Large Underground Xenon (LUX) Experiment.*

[arXiv:1211.3788 \[physics.ins-det\]](https://arxiv.org/abs/1211.3788)

The LUX Collaboration, *Radiogenic and Muon-Induced Backgrounds in the LUX Dark Matter Detector.*

[arXiv:1403.1299 \[astro-ph.IM\]](https://arxiv.org/abs/1403.1299)

The LUX Collaboration, *First results from the LUX dark matter experiment at the Sanford Underground Research Facility.* [arXiv:1310.8213 \[astro-ph.CO\]](https://arxiv.org/abs/1310.8213)

Klute M., *Lecture notes from 8.811*. Fall 2015

PDG Particle Review, *Plots of cross sections and related quantities*. 2015

PDG Particle Review, *CKM quark-mixing matrix*. 2015

Smirnov A. Y., *The MSW effect and Solar Neutrinos*. [arXiv:hep-ph/0305106](https://arxiv.org/abs/hep-ph/0305106)

Tapper A., *High Q^2 neutral current cross sections in $e^- p$ DIS.*

<http://www.hep.ph.imperial.ac.uk/~tapper/talks/dis04.pdf>

Thomson M., *Modern Particle Physics*

Thomson M., *Online lecture notes*
(<http://www.hep.phy.cam.ac.uk/~thomson/partIIIparticles/welcome.html>)

Undagoitia T., Ludwig R., *Dark matter direct-detection experiments.* arXiv:1509.08767 [physics.ins-det]

Universitat Heidelberg, *Solar neutrino problem.*
http://www.kip.uni-heidelberg.de/tt_detektoren/neutrinos.php?lang=en

Wong S. S. M., *Introductory Nuclear Physics.*